SECURITY CLASSIFICATION OF THIS PAGE (When Data Entered)

REPORT DOCUMENTATION PAGE

READ INSTRUCTIONS BEFORE COMPLETING FORM

1. REPORT NUMBER: AD56471
2. GOVT ACCESSION NO.
3. RECIPIENT'S CATALOG NUMBER

4. TITLE (and Subtitle): (6) EXCIMER POTENTIAL CURVES (12) (9)

5. TYPE OF REPORT & PERIOD COVERED: Annual Report No. 2, 1 Jan [redacted] 31 Dec [redacted]78

6. PERFORMING ORG. REPORT NUMBER

7. AUTHOR(s): (10) H. S. Taylor, M. Valley, C. Watts

8. CONTRACT OR GRANT NUMBER(s): (15) N0014-77-C-0102, ARPA Order-2840

9. PERFORMING ORGANIZATION NAME AND ADDRESS: University of Southern California, Los Angeles, California 90007

10. PROGRAM ELEMENT, PROJECT, TASK AREA & WORK UNIT NUMBERS: (11) Mar 79, NR395-570

11. CONTROLLING OFFICE NAME AND ADDRESS: Office of Naval Research, 800 N. Qunicy Street, Arlington, Virginia 22217

12. REPORT DATE: March 1, 1979

13. NUMBER OF PAGES: 42 (12) 42 p.

14. MONITORING AGENCY NAME & ADDRESS (if different from Controlling Office)

15. SECURITY CLASS. (of this report): Unclassified

15a. DECLASSIFICATION/DOWNGRADING SCHEDULE

LEVEL III

16. DISTRIBUTION STATEMENT (of this Report): Unlimited

DISTRIBUTION STATEMENT A
Approved for public release;
Distribution Unlimited

DDC
RECEIVED
MAR 21 1979
C

17. DISTRIBUTION STATEMENT (of the abstract entered in Block 20, if different from Report)

18. SUPPLEMENTARY NOTES

19. KEY WORDS (Continue on reverse side if necessary and identify by block number)

Excimers
potential curves
random phase approximation
configuration interaction calculation
Effective potential
laser
GaKr
LiHe

20. ABSTRACT (Continue on reverse side if necessary and identify by block number)

This report describes the present status of our effort to develop and implement semi-empirical and theoretical methods for obtaining potential curves of diatomic excimer systems. The basic theory of the semi-empirical electorn scattering model is reviewed and the results of preliminary calculations on LiHe are presented.

DD FORM 1 JAN 73 1473 EDITION OF 1 NOV 65 IS OBSOLETE
S/N 0102-LF-014-6601

SECURITY CLASSIFICATION OF THIS PAGE (When Data Entered)

Annual Report #2

January 1, 1978 - December 31, 1978

EXCIMER POTENTIAL CURVES

Contract No. N00014-77-C-0102
ARPA Order No. 2840

H. S. Taylor, Principal Investigator

(213) 741-2590

M. Valley
C. Watts

University of Southern California
University Park
Los Angeles, California 90007

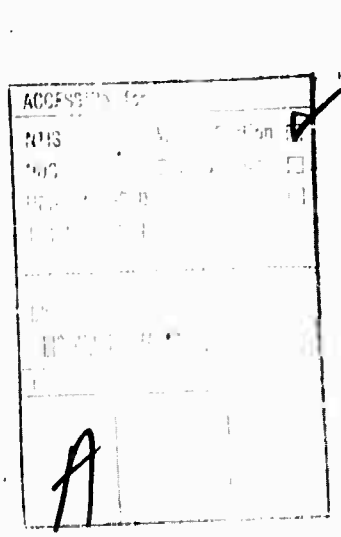

I. Introduction

This Annual Scientific Report covers work performed under Contract No. N00014-77-C-0102, entitled Excimer Potential Curves. This report describes the present status of our effort to develop and implement semi-empirical and theoretical methods for obtaining potential curves of diatomic excimer systems. Our emphasis is on developing and testing methods which will be reasonably accurate yet will not require long lead times for development and will not require excessive amounts of computer time for production runs. The final objective is to enable experimentalists to choose or reject possible laser systems on the basis of inexpensive theoretical calculations rather than on the basis of expensive and time-consuming experiments.

We are particularly interested in developing methods that are applicable to excimer systems because of the current emphasis on these systems as candidates for efficient, high-power visible and ultraviolet lasers. After consultation with A.V. Phelps and A. Gallagher of J.I.L.A., we decided to concentrate initially on molecules of rare gases with Thallium, Indium or Gallium..

In the first annual report for this contract[1] (referred to as AR1) we presented Configuration Interaction (CI) calculations on GaKr and used these results to extrapolate to potential curves for InKr and TlKr. These potential curves were then used to predict the spontaneous emission and absorption coefficients for these systems. Since the first annual report, the numerical procedure used to calculate these coefficients has been refined and the revised results were published in the Journal of Chemical Physics[2]; a copy of this paper is included as appendix A.

For systems with a large number of electrons, such as Tl-R (R is a rare gas atom), present CI programs are inadequate and offer no hope of extension in the immediate future. Consequently, our effort is concentrated on developing and testing semi-empirical methods that can easily and rapidly be applied to the excimer systems of interest. This report covers our progress in this area.

The basic theory for the effective potential method was described in detail in the first annual report and will be reviewed only briefly in section II. In order to implement the effective potential method, we have had to develop a new molecular integral package. Because of the complexity of these integrals, we used an algebraic programming routine, REDUCE,[3] to evaluate the analytic expressions needed. Details of this procedure are described in Section III. At the present time we are testing the first phase of our effective potential program package on LiHe. Results of our preliminary calculations are presented and discussed in Section IV.

II. The Effective Potential Method

This section briefly reviews the theoretical basis of our calculations using the effective potential method. For an excimer system AB, where A is a closed-shell system, most of the states of interest correspond to the asymptotic situations where B is excited but A is in its ground state. Fundamentally, what the effective potential theory says is that any charged particle in B sees a potential (Σ_A), due to the closed-shell system A, which is the same as if the charged particle were scattered off of A. This scattering potential is corrected for the fact that A is "de-polarized" relative to the scattering problem, due to the presence of the nucleus and other electrons of B. This theory is based on the model interaction potentials and response functions that arise out of the many body theory (using Schwinger Functional Derivatives) and that have been applied to scattering problems.[4]

Using many-body field theoretic methods it has been shown that the change in energy, ε, resulting from the addition of an electron to a closed-shell reference system (referred to here as A) is given by the one-particle Dyson equation

$$T(r)\phi(r) + \int dr' \; \Sigma^A(r;r':\varepsilon)\phi(r) = \varepsilon\phi(r) \qquad (1)$$

where T is the kinetic energy operator and ϕ is the Dyson amplitude with r and r' being space-spin coordinates. Thus, the problem reduces to an effective one-particle problem in which this particle experiences an effective potential, Σ^A, which represents all the other particles collectively, taking into account all effects such as polarization, correlation and exchange, etc. As might be expected, the cost of this simple formulation is that Σ^A is an extremely complicated entity which is both nonlocal and energy dependent and which cannot rigorously be brought into closed form. However, it has been possible to

develop excellent closed form approximations to this potential which are based on well founded physical concepts. Most notable among these is the Random Phase Approximation (RPA) potential, Σ_{RPA}, which has been very successfully used in calculating the ionization potentials, excitation energies, oscillator strengths, and elastic-scattering phase shifts for He[5]. Σ_{RPA} has also been used to accurately calculate the ionization and excitation energies of Li[6]. Moreover, it has been shown that this ab initio potential encompasses other phenomenologically derived semiemperical potentials which have been used by other workers with great success[7].

In the first annual report we showed how the same many-body techniques could be applied to the problem of adding m_e electrons and m_n nuclei of mass M_i^B to a closed-shell reference system (A). By assuming that 1) all three-particle and higher potentials can be neglected, and 2) the non-adiabatic, energy dependent potentials can be replaced by their hermitian, energy independent, adiabatic approximatis, we separated the electronic and nuclear motion and obtained the following equations. We take system B to consist of m_e electrons and m_n nuclei with a fixed internuclear geometry. The intermolecular potential of the system A-B as a function of the separation between A and B is then

$$V_B^A(R) = E_B^A(R) - E_B^\circ + V_{B,nuc}^A(R) \qquad (2)$$

where

$$V_{B,nuc}^A(R) = -\sum_{i=1}^{m_n} \Sigma^A(R_i : Z_i^B ; M_i^B) + \sum_{i>j}^{m_n} W^A(R_i, R_j : Z_i^B, Z_j^B), \qquad (3)$$

and where

$$E_B^\circ = \mathcal{E}_B^\circ + \sum_{i>j}^{m_n} \frac{z_i^B z_j^B}{|R_i - R_j|} \tag{4}$$

is just the electronic energy of isolated system B and where $E_B^A(R)$ is given by

$$\left[H(r_1 \ldots r_{m_e}; R) + \sum_{i=1}^{m_e} \int dr_i' \left(\Sigma^A(r_i; r_i': 1; 1) - \sum_{j=1}^{m_n} W^A(r_i, R_j; r_i': 1, z_j^B) \right) \right.$$

$$\left. + \sum_{i>j}^{m_e} \int dr_i' dr_j' \, W^A(r_i, r_j; r_i', r_j': 1, 1) \right] \Psi_B^A(r_1 \ldots r_{m_e}) = E_B^A(R) \, \Psi_B^A(r_1 \ldots r_{m_e}) . \tag{5}$$

H is the usual hamiltonian for m_e electrons in the field of m_n fixed nuclei:

$$H(r_1 \ldots r_{m_e}; R) = \sum_{i=1}^{m_e} \left(T(r_i) - \sum_{j=1}^{m_n} \frac{z_j^B}{|r_i - R_j|} \right) + \sum_{i>j}^{m_e} \frac{1}{|r_i - r_j|}$$

$$= \sum_{i=1}^{m_e} h(r_i) + \sum_{i>j}^{m_e} \frac{1}{r_{ij}} \quad . \tag{6}$$

W^A is a two-particle effective potential which represents how the presence of one particle affects the potential seen by the other particle and which reflects the fact that system A can act as a dielectic medium to shield the Coulombic interaction between two charged particles.

Therefore, given that we know E_B°, we are left with two problems. The first is to obtain good closed form adiabatic approximates for Σ^A and W^A, and the second is to find the solutions of equation 5. Various means of solving these problems were discussed in AR1. In the remainder of this section we will outline the procedure we are using.

The one- and two-particle effective potentials Σ^A and W^A appearing in equation 5 are hermitian adiabatic approximates to the true field theoretic potentials. As we have mentioned, such potentials can be obtained in closed

ab initio form using many-body theory within the framework of the RPA approximation and taking the adiabatic limits. However, while these potentials are tractable they are nonetheless quite complicated and their use would entail considerable computational effort. In view of the perturbative nature of our theory it is reasonable to expect that we could use potentials having simpler forms. Such simpler potentials can be obtained by making moment expansions of the RPA potentials and truncating these expansions in a physically meaningful manner[8]. When this is done, the resulting potentials can be cast in forms which are very similar to phenomenologically derived semiempirical potentials which have been used by other workers with condiderable success[9]. Therefore, it would seem that the use of complicated ab initio potentials is not warranted (although we do reserve the option to do so) and that we can take our potentials to have semiempirical forms similar to those used by Dalgarno and by Victor[9], namely

$$\int dr' \Sigma^A(r;r':z;M) = -\frac{Z^A}{r} + \int dr' \Sigma^A_{HF}(r;r';z) - \frac{\alpha_d^A Z^2}{2r^4} W_6(kr) - \frac{Z^2(\alpha_q^A - \frac{6\beta_1}{M})}{2r^6} W_8(kr) + Z^2(a_0 + a_1 r + a_2 r^2) e^{-kr} \qquad (7)$$

and

$$\int dr_1' dr_2' W^A(r_1, r_2; r_1', r_2': Z_1 Z_2) = -\frac{\alpha_d^A Z_1 Z_2}{r_1^2 r_2^2} W_3(kr_1) W_3(kr_2) P_1(\cos\gamma_{12}) - \frac{\alpha_q^A Z_1 Z_2}{r_1^3 r_2^3} W_4(kr_1) W_4(kr_2) P_2(\cos\gamma_{12}), \qquad (8)$$

where we have chosen our coordinate system to be centered on A which for simplicity we now take to be an atom having a nuclear charge of z^A

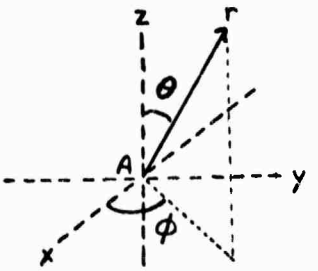

and where

$W_n(x)$ = $(1-e^{-x^n})$ is a cutoff function

γ_{12} = angle between vectors r_1 and r_2

$P_\ell(x)$ = legendre polynomial of the ℓ^{th} degree

α_d^A = dipole polarizability of A

α_q^A = approximate quadrupole polarizability of A (adjustable)

β_1 = dynamic correction constant

k = approximately 1/2 r_o where r_o is the effective radius of A (adjustable)

$\{a_i\}$ = adjustable monopole parameters

and

$$\Sigma_{HF}^A(r;r') = \sum_{i=1}^{n_A} \frac{\Phi_i^{A*}(r')[2-P_{r,r'}]\,\Phi_i^A(r')}{|r-r'|} \qquad (9)$$

is the static Hartree-Fock potential of A with $\{\phi_i^A\}$ being the n_A spatial Hartree-Fock orbitals for the electrons in A . $P_{r,r'}$ is the permutation operator if r is an electronic coordinate whereas $P_{r,r'} = 0$

if r is a nuclear coordinate. Note that all quantities are now purely spatial and that Σ^A and W^A are therefore explicitly spin independent.

In (7) the first term is simply the potential due to the nucleus of A and the second term is the static Hartree-Fock potential for the electrons in A occupying the spatial orbitals $\{\phi_i^A\}$. The next two terms in (7) are asymptotically correct induced dipole and quadrupole polarization potentials which die off rapidly at short distances from A. The term in β_1 describes dynamic effects and is negligible when R is a nuclear coordinate. The final term is an induced monopole term[7,8] which also serves as a short range correction potential. In the calculations of Dalgarno and of Victor[9] these short range terms are combined with a pseudopotential. The terms in (8) describe an asymptotically correct dielectric potential which properly cancels out one-particle induced dipole and quadrupole polarizations of A due to two particles of the same charge when these particles are on opposite sides of A. That these potentials represent a significant simplification over the ab initio potentials is clear in that our two-particle potential is strictly local and the only nonlocal term in the one-particle potential is simply the usual Hartree-Fock exchange potential. However, despite their simplicity, potentials such as these have been used very successfully for a variety of problems in the past and should therefore be quite adequate for our purposes.

As was demonstrated in AR1, the two-particle potential of equation 8, can be written in terms of one-particle operators only:

$$\int dr_1' dr_2' \, W^A(r_1, r_2; r_1', r_2') = -\sum_{i=1}^{8} Q_i(r_1) Q_i(r_2) \qquad (10a)$$

where

$$
\begin{aligned}
Q_1(r) &= \sqrt{\alpha_d^A}\,|r|^{-2}W_3(k|r|)P_1(\cos\theta)\\
Q_2(r) &= \sqrt{\alpha_d^A}\,|r|^{-2}W_3(k|r|)\,P_1^1(\cos\theta)\cos\phi\\
Q_3(r) &= \sqrt{\alpha_d^A}\,|r|^{-2}W_3(k|r|)\,P_1^1(\cos\theta)\sin\phi\\
Q_4(r) &= \sqrt{\alpha_q^A}\,|r|^{-3}W_4(k|r|)\,P_2(\cos\theta)\\
Q_5(r) &= \sqrt{1/3}\sqrt{\alpha_q^A}\,|r|^{-3}W_4(k|r|)\,P_2^1(\cos\theta)\cos\phi\\
Q_6(r) &= \sqrt{1/3}\sqrt{\alpha_q^A}\,|r|^{-3}W_r(k|r|)\,P_2^1(\cos\theta)\sin\phi\\
Q_7(r) &= \sqrt{1/12}\sqrt{\alpha_q^A}\,|r|^{-3}W_4(k|r|)\,P_2^2(\cos\theta)\cos 2\phi\\
Q_8(r) &= \sqrt{1/12}\sqrt{\alpha_q^A}\,|r|^{-3}W_4(k|r|)\,P_2^2(\cos\theta)\sin 2\phi
\end{aligned}
\qquad (10b)
$$

Given a set of semi-empirical parameters for the effective potential, we solve equation 5 by variational methods. Solutions can be obtained at two levels of complexity, analagous to SCF and CI calculations on atom B in the presence of an external potential representing atom A.

The remaining problem is to obtain values of the semi-empirical parameters. We intend to solve this problem by applying the perturbation treatment given in AR1. We showed that the first-order perturbative expression for V_B^A is simply

$$V_B^A = V_{B,nuc}^A + \langle \Psi_B^\circ | U^A | \Psi_B^\circ \rangle \qquad (11)$$

where

$$U^A(r_1 \ldots r_{m_e}; R) = \sum_{i=1}^{m_e} \int dr_i' \left[\Sigma^A(r_i; r_i' : z_i; M_i) + \sum_{j=1}^{m_n} W^A(r_i, R_j; r_i' : z_i Z_j^B) \right]$$
$$+ \sum_{i>j}^{m_e} \int dr_i' dr_j' W^A(r_i, r_j; r_i', r_j' : z_i, z_j)$$
$$= \sum_{i=1}^{m_e} p^A(r_i) + \sum_{i>j}^{m_e} q_{12}^A(r_i, r_j) \qquad (12)$$

and Ψ_B° is the wavefunction for isolated system B. We assume that we know some potential curve, from experiments or calculations for the interaction of A with B'. We can then use this known curve and equation 11 to fit the parameters for U^A. If we assume that U^A is not a function of B', we can use this potential to calculate V_B^A for other atoms B or for other states of B'. In the following section we return to the problem of solving equation 5 with an assumed form for the effective potential.

III. Details of the Calculation

In developing a program package to implement the effective potential method, our goal was to make the package as general as possible. To achieve this, we have made our effective potential program EFFPOT compatible with the GVB II[10] SCF and CI programs. This program package is a gaussian basis function, molecular SCF and CI routine which will enable the present version of EFFPOT to be extended to large molecules. The version of GVB II that we are using has an option for replacing the atomic cores by a pseudopotential; however, the form of this built-in pseudopotential is different from those being developed for large atoms[11]. The modifications needed to make use of available pseudopotentials would be relatively easy.

The GVB II progam package consists of a number of sequential program steps which are outlined below.

1. Integral generation	a) PLYLABS -	creates list of unique integral labels
	b) PLYINTS -	evaluates integrals
2. Integral preprocessing	a) PLYIJLK, b) PLYPAIR	convert output of PLYINTS to form needed for input to GVB II
3. SCF	GVB II	
4. CI	a) CORTRN	transforms to molecular basis
	b) CIPROG	

To perform an effective potential calculation, the program EFFPOT is inserted between steps 2a and 2b.

EFFPOT calculates the additonal integrals required, $\langle\phi_i|\Sigma^A|\phi_j\rangle$ and $\langle\phi_i|Q_n|\phi_j\rangle$ (see equations 7-10), and modifies the integral tape so that the insertion of an effictive potential is transparent to GVB II. These integrals have not been previously evaluated for gaussian basis sets, and because of the cut-off functions in Σ^A and Q_n and the angular dependence of Q_n, the evaluation of these integrals is rather complicated, especially for two-center integrals containing basis functions for $\ell > 0$.

Although it is relatively easy to construct an algorithm for evaluating these integrals, the algebraic detail rapidly becomes overwhelming. To alleviate this problem, we used the algebraic programming system REDUCE[3] to produce the FORTRAN code required to evaluate these integrals. An explanation of the algorithm used to derive the integral expressions and an example of the input to REDUCE are given below for one of the more complicated integrals.

The integral we shall consider is

$$\langle P_x^E | Q_4^B | P_x^F \rangle \tag{13}$$

where the superscripts indicate the atomic center on which the (basis or potential) function is centered, Q_4 is defined by equation 10b and P_x indicates a "p_x" gaussian basis function. This integral can be written explicitly as

$$\langle P_x^E | Q_4^B | P_x^F \rangle =$$

$$\sqrt{\alpha_q^A/3} \int d\tau\, x_E\, e^{-\alpha r_E^2}\, r_B^{-3}\, W_4(kr_B) P_2(\cos\theta_B)\, x_F\, e^{-\beta r_F^2}$$

$$= \sqrt{\alpha_q^A/3}\; I. \tag{14}$$

Using the relation

$$P_2(\cos\theta_B) = \frac{3z_B^2 - r_B^2}{2r_B^2}, \tag{15}$$

we can write

$$I = \frac{3}{2}\int d\tau\, x_E e^{-\alpha r_E^2} W_4(kr_B) z_B^2 r_B^{-5} x_F e^{-\beta r_F^2} - \frac{1}{2}\int d\tau\, x_E e^{-\alpha r_E^2} W_4(kr_B) r_B^{-3} x_F e^{-\beta r_F^2}$$

$$\equiv I_1 + I_2. \tag{16}$$

In order to obtain the term z_B^2, we will set up a fake gaussian on center B, $e^{-cr_B^2}$, and move the $W4(kr_B)/r_B^5$ term to a fake center, D; after evaluating the resulting integral, we will take the limits D → B and c → 0. Using the relation

$$z_B^2 e^{-cr_B^2} = \frac{1}{2^2c^2}\frac{\partial^2}{\partial B_z^2} e^{-cr_B^2} + \frac{1}{2c} e^{-cr_B^2}, \tag{17}$$

we obtain

$$I_1 = \lim_{c\to 0}\lim_{D\to B} \frac{3}{2}\frac{1}{2^2\alpha\beta}\frac{\partial^2}{\partial E_x \partial F_x}\left\{\frac{1}{2^2c^2}\frac{\partial^2}{\partial B_z^2} I_3 + \frac{1}{2c} I_3\right\} \tag{18}$$

where

$$I_3 = \int d\tau\, e^{-\alpha r_E^2} e^{-cr_D^2} r_D^{-5} W_4(kr_D) e^{-\beta r_F^2}. \tag{19}$$

We can also write

$$I_2 = \frac{-1}{2^3\alpha\beta}\frac{\partial^2}{\partial E_x \partial F_x} I_4 \tag{20}$$

where

$$I_4 = \int d\tau\, e^{-\alpha r_E^2} e^{-\beta r_F^2} r_B^{-3} W_4(kr_B). \tag{21}$$

We can then apply the rule for combining gaussians on two centers,

$$e^{-\alpha r_E^2} e^{-\beta r_F^2} = e^{-\frac{\alpha\beta}{\gamma} R_{EF}^2} e^{-\gamma r_A^2} \tag{22}$$

where $\gamma = \alpha + \beta,$ (22a)

REF is the distance between centers E and F, and center A is defined by

$$A_x = (\alpha E_x + \beta F_x)/\gamma. \tag{22b}$$

We then use the Fourier Convolution Theorem to obtain the following expressions for I_3 and I_4:

$$I_3 = e^{-\frac{\alpha\beta}{\gamma} R_{EF}^2} e^{-\frac{\gamma\delta}{\delta} R_{AD}^2} I_5 \tag{23}$$

where

$$I_5 = \int d\tau\, e^{-\delta r_G^2} r_D^{-5} W_4(kr_D) \tag{24}$$

$$= \frac{\pi}{\delta R_{DG}} \int_0^\infty dr\, r^{-4} W_4(kr) \left\{ e^{-\delta(r-R_{DG})^2} - e^{-\delta(r+R_{DG})^2} \right\},$$

and

$$I_4 = e^{-\frac{\alpha\beta}{\gamma} R_{EF}^2} I_6 \tag{25}$$

where

$$I_6 = \int d\tau\, e^{-\gamma r_A^2} r_B^{-3} W_4(kr_B) \tag{26}$$

$$= \frac{\pi}{\delta R_{AB}} \int_0^\infty dr\, r^{-2} W_4(kr) \left\{ e^{-\gamma(r-R_{AB})^2} - e^{-\gamma(r+R_{AB})^2} \right\}.$$

In these equations $\delta = \gamma + c$ and G is the center obtained by combining Gaussians on A and D. The derivatives and limits in equation 18 are obtained analytically by REDUCE and the result is that equation 18 is written as a sum of integrals with forms similar to those given by equations 24 and 26. These basic integrals are evaluated numerically and summed to give the result for $\langle P_X^E | Q_4^B | P_X^F \rangle$. To obtain expressions for this integral in the case where any of centers E,F,B coincide, REDUCE is used to obtain the appropriate limit ($E \to F$, for example). The REDUCE commands used to evaluate all Q_4 integrals are given in Appendix B. The output from this REDUCE code is rearranged, using additional REDUCE commands, to produce FORTRAN code which can be inserted directly in the integral evaluation subroutines.

The present versions of the EFFPOT integral routines are restricted to two centers and s or p basis functions. Our tests of this program on LiHe are described in the next section.

IV Test Calculations on LiHe

In this section we present the results of the first stage of our tests of the effective potential method. We have chosen LiHe as the test system, and in this stage of the tests we assume that the parameters of our semi-empirical potential are known.

Values of α_d and α_q can easily be obtained; however, it should be pointed out that in a semi-empirical potential, each parameter plays a dual role. Besides describing the physical effect to which it most obviously corresponds, each parameter also serves to correct for the deficiencies of the semi-empirical model. Consequently in the best fit for the potential parameters, the values of α_d, α_q, etc., should not be expected to equal the physical quantities. The values for the cut-off functions and for the short-range part of the potential are harder to obtain. Our initial desire was to use the parameters obtained by Peach.[12] She calculated the parameters for a model potential describing one electron outside of He by fitting the parameters to electron-He atom scattering data. Her model also included a pseudopotential to represent the Hartree-Fock potential of He; this fact makes it impossible to separate the pseudopotential from the short-range terms needed for the effective potential (see equation 7). Consequently, for our test calculations, we use Peach's values for α_d, α_q', β and her cut-off functions. In addition, we have guessed a value for a_o (equation 7), so that the short-range potential has only one term.

The exact forms of the potentials used in our test calculations are

$$\int dr' \Sigma^A(r;r':z) = \frac{Z^A z}{r} + z\int dr' \Sigma^A_{HF}(r;r') + z^2 a_0 e^{-\gamma r} - \frac{\alpha_d z^2}{2r^4} W_2(\beta r) - \frac{\alpha' z^2}{2r^6} W_3(\beta' r) \quad (27)$$

$$\int dr_1' dr_2' W^A(r_1,r_2;r_1',r_2':z_1,z_2) = \frac{-\alpha_d z_1 z_2}{2 r_1^2 r_2^2} X_2(\beta r_1) X_2(\beta r_2) P_1(\cos\gamma_{12}) - \frac{\alpha_q' z_1 z_2}{2 r_1^3 r_2^3} X_3(\beta r_1) X_3(\beta r_2) P_2(\cos\gamma_{12}) \quad (28)$$

Where W_n is defined by

$$W_n(x) = [X_n(x)]^2 \quad (29a)$$

and

$$X_n(x) = 1 - \exp(-x)\sum_{m=0}^{n} \frac{x^m}{m!} \underset{x\to 0}{\approx} \frac{x^{n+1}}{(n+1)!} \quad (29b)$$

$$\alpha' = (\alpha_q' - 6\beta_1/M).$$

The values of the parameters used are given in table 1.

In tables 2 and 3 and figures 1 and 2, we compare the effective potential-SCF (EP-SCF) calculations with SCF[13] and restricted CI calculations for the same basis set. The basis set is that of Krauss, Maldonado and Wahl[13]. We have not yet completed the effective potential-CI (EP-CI) or full CI calculations. The restricted CI claculations presented here have the same aymptotic limit as the EP-CI calculations, but do not fully allow for distortion of He at intermediate distances. In comparing these results, it should be noted that the EP-SCF results have the same $R \to \infty$ limit as the SCF calculation, but that at intermediate distances, the EP-SCF results go as $1/R^6$ while the SCF calculations cannot give this dependence. Also, the full CI claculations, which allow for more He polarization, should give more attractive interaction

Table 1. Parameters for the potential defined by equations 27 to 29, for He[a]

Z_a	2.
a_o	.05
γ	1.59
α_d	1.3834
β	2.09928
α'	-2.1222
β'	0.551429
α'_q	2.11380

[a]All the parameters except a_o and γ are taken from Peach.[12]

Table 2. LiHe total energies (in Hartrees)

	EP-SCF		SCF[a]		CI (restricted)	
R(a.u.)	$^2\Sigma$	$^2\Pi$	$^2\Sigma$	$^2\Pi$	$^2\Sigma$	$^2\Pi$
2.	-10.19137	-10.14751	-10.18797	-10.14029	-10.20229	-10.15458
3.	-10.27436	-10.22475	-10.27465	-10.22372	-10.29037	-10.23938
4.	-10.28454	-10.22723	-10.28397	-10.22646	-10.29993	-10.24232
5.	-10.28933	-10.22603	-10.28840	-10.22546	-10.30449	-10.24138
6.	-10.29166	-10.22533	-10.29113	-10.22500	-10.30722	-10.24090
8.	-10.29321	-10.22486	-10.29304	-10.22477	-10.30911	-10.24067
10.	-10.29339	-10.22476	-10.29335	-10.22473	-10.30944	-10.24065

[a]Krauss, Maldonado, and Wahl[13]

Table 3. LiHe interaction enrgies (in Hartrees)

	EP-SCF		SCF[a]		CI(restricted)		Full CI	
R(a.u.)	$^2\Sigma$	$^2\Pi$	$^2\Sigma$	$^2\Pi$	$^2\Sigma$	$^2\Pi$	$^2\Sigma$	$^2\Pi$
2.	.10201	.07735	.10541	.08457	.10723	.09608		
3.	.01902	-.00004	.01873	.00099	.01915	.00128	.02000	
4.	.00884	-.00252	.00941	-.00175	.00959	-.00166		
5.	.00405	-.00132	.00498	-.00075	.00503	-.00072		
6.	.00172	-.00062	.00225	-.00029	.00230	-.00024		
8.	.00017	-.00015	.00034	-.00006	.00041	-.00001		
10.	-.00001	-.00005	.00004	-.00002	.00008	.00001		

[a] Krauss, Maldonado, and Wahl[13]

References

1. H.S. Taylor, M. Valley, C. Watts, and F. Bobrowicz, "Excimer potential curves," Annual Report No. 1, ARPA contract no. N00014-77-C-0102, Feb. 1, 1978.

2. T.H. Dunning, Jr., M. Valley and H.S. Taylor, J.Chem Phys. 69, 2672 (1978).

3. A.C. Hearn, REDUCE 2 Users's Manual, Second Edition, 1974.

4. B. Schneider, H.S. Taylor and R. Yaris, Phys. Rev. A1, 855 (1970), G. Csanak and H.S. Taylor, Phys. Rev. A6, 1843 (1972).

5. B.S. Yarlagadda, G. Csanak, H.S. Taylor, B. Schneider and R. Yaris, Phys. Rev. A7, 146 (1973); L.D. Thomas, G. Csanak, H.S. Taylor and B.S. Yarlagadda, J. Phys. B7, 1719 (1974).

6. B. Schneider, H.S. Taylor, R. Yaris, and B.S. Yarlagadda, Chem. Phys. Letters 22, 381 (1973).

7. G. Csanak and H.S. Taylor, Phys. Rev. A6, 1843 (1972); G. Csanak and H.S. Taylor, J. Phys. B6, 2055 (1973).

8. S.W. Wang, H.S. Taylor and R. Yaris, Chem. Phys. 14, 53 (1976).

9. A. Dalgarno, C. Bottcher and G.A. Victor, Chem. Phys. Lett. 7, 265 (1970), C. Bottcher and A. Dalgarno, Proc. R. Soc. Lond. A 340 187 (1974); D.K. Watson, C.J. Cerjan, S. Guberman and A. Dalgarno, submitted to Chem. Phys. Lett. 1977.

   C. Laughlin and G.A. Victor, Atomic Physics 3, 247 (1973).

10. N.W. Winter, F.W. Bobrowicz and W.A. Goddard III, J. Chem. Phys. 62 4325 (1975).

11. Y.S. Lee, W.C. Ermler and K.S. Pitzer, J. Chem. Phys. 67, 5861 (1977) W.R. Wadt, P.J. Hay and L.R. Kahn, J. Chem. Phys. 68 1752 (1978).

12. G. Peach, J. Phys. B 11, 2107 (1978).

13. M. Krauss, P. Maldonado and A.C. Wahl, J. Chem. Phys. 54, 4944 (1971).

Figure Captions

1. Interaction energy for LiHe $^2\Sigma$ state.

   ⊙ connected by solid line; EP-SCF results.

   ⊡ SCF results of Krauss, Maldonado, and Wahl[13].

   · restricted CI calculation.

2. Interaction energy for LiHe $^2\Pi$ state.

   ⊙ connected by solid line; EP-SCF results.

   ⊡ SCF results of Krauss, Maldonado, and Wahl[13].

   · restricted CI calculation.

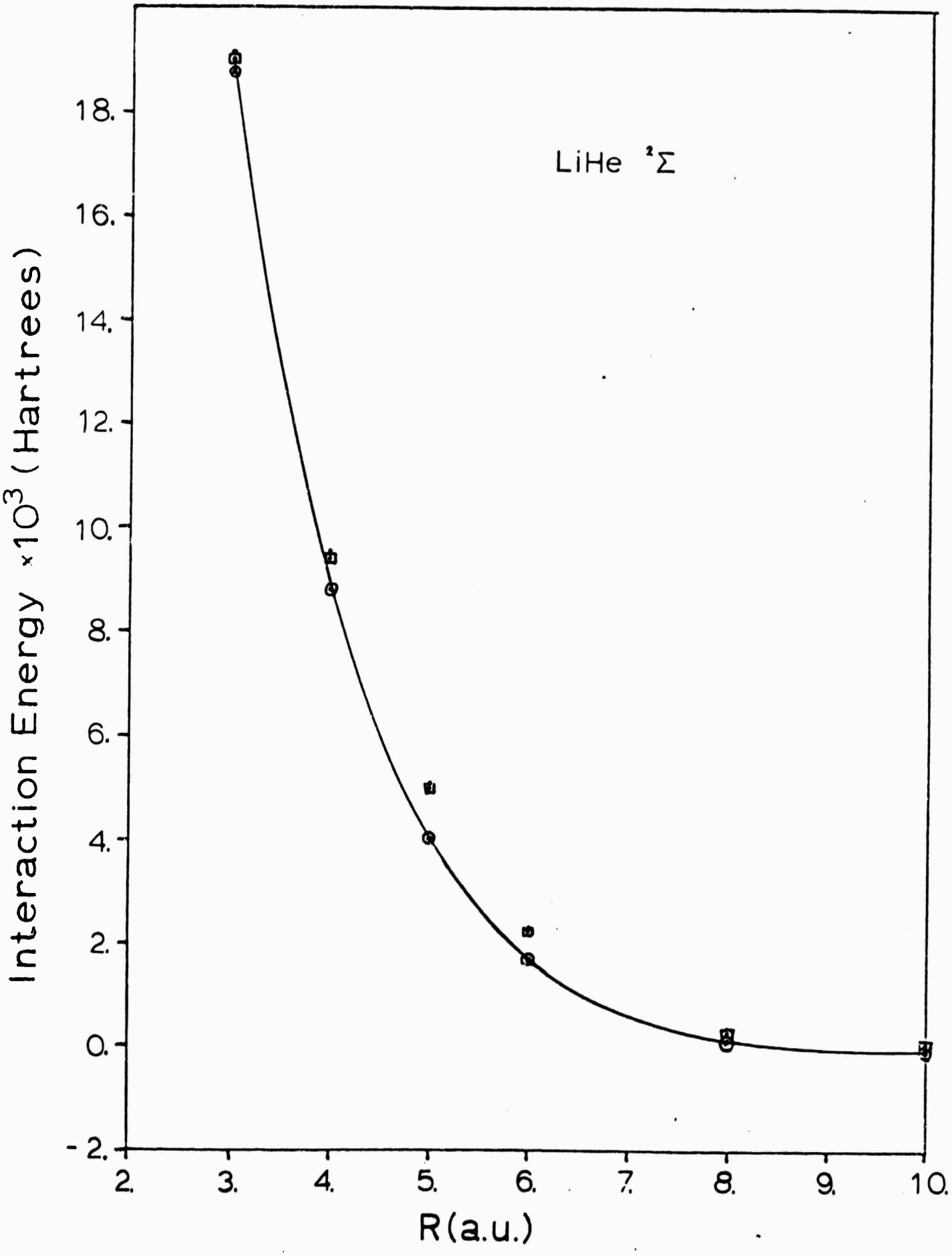
LiHe $^2\Sigma$
Interaction Energy $\times 10^3$ (Hartrees)
18.
16.
14.
12.
10.
8.
6.
4.
2.
0.
- 2.
2.
3.
4.
5.
6.
7.
8.
9.
10.
R(a.u.)

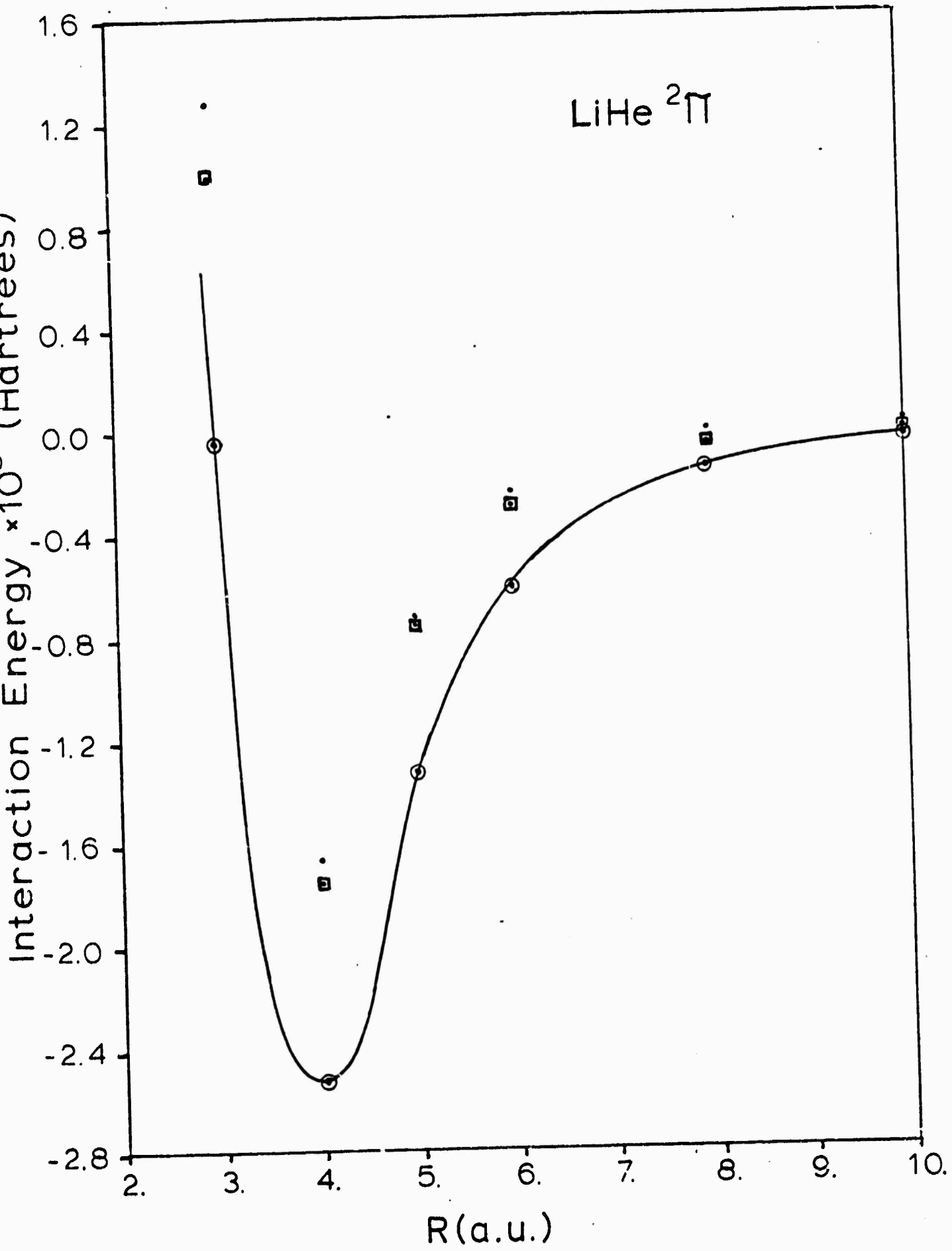
LiHe $^2\Pi$
Interaction Energy $\times 10^3$ (Hartrees)
1.6
1.2
0.8
0.4
0.0
-0.4
-0.8
-1.2
-1.6
-2.0
-2.4
-2.8
2.
3.
4.
5.
6.
7.
8.
9.
10.
R(a.u.)

Appendix A

Theoretical studies of the low-lying electronic states of GaKr, including extrapolation to InKr and TlKr[a)]

Thom. H. Dunning, Jr.[b)]

Chemistry–Nuclear Chemistry Division, Los Alamos Scientific Laboratory, Los Alamos, New Mexico 87545

Marcy Valley and Howard S. Taylor

Department of Chemistry, University of Southern California, Los Angeles, California 90007
(Received 25 April 1978)

We report *ab initio* configuration interfaction calculations on the states of the gallium krypton (GaKr) molecule arising from the $Ga(^2P_{1/2,3/2},{}^2S_{1/2}) + Kr(^1S_0)$ and $Ga^+(^1S_0) + Kr(^1S_0)$ separated atom limits. The potential energy curves for the states arising from the $Ga(^2P_{1/2,3/2})$ limits, the *I* 1/2, *II* 1/2, and *i* 3/2 states, are found to be repulsive. The potential energy curves for the states arising from the $Ga(^2S_{1/2})$ and $Ga^+(^1S_0)$ limits, the *III* 1/2 and 1 0 states, are both found to be weakly bound; D_e (*III* 1/2) = 0.047 eV and D(1 0) = 0.24 eV. The potential energy curves and transition moments obtained in the GaKr calculations have been used to simulate the curves and moments for InKr and TlKr. Using this data the absorption and emission coefficients of all three molecules have been calculated.

I. INTRODUCTION

The Group IIIA-rare gas excimer molecules are considered to be attractive candidates for developing an efficient, high power, tunable laser in the visible region of the spectrum.[1] The transition under consideration is a perturbed $(n+1)^2S_{1/2}$–$n^2P_{1/2,3/2}$ transition of the Group IIIA atom. While current experimental studies have concentrated on the thallium-rare gas systems, especially TlXe, as the most promising candidates, Gallagher[2] has recently raised the possibility of using the gallium-rare gas systems by obtaining gallium atoms from the dissociation of GaI_3.

To provide further information on the nature of the excimer states involved in these studies, we report here *ab initio* configuration interaction calculations on a prototype Group IIIA-rare gas diatomic molecule, GaKr. We present the potential energy curves for all of the states arising from the neutral $Ga(^2P_{1/2,3/2}, {}^2S_{1/2}) + Kr(^1S_0)$ and ionic $Ga^+(^1S_0) + Kr(^1S_0)$ separated atom limits and the dipole transition moments radiatively coupling the states. We then use the computed potential curves and transition moments for GaKr, along with the experimental atomic spin-orbit coupling constants, to model the curves and moments for InKr and TlKr. With this data we calculate the emission and absorption coefficients for all three systems using the classical technique developed by Gallagher and co-workers.[16]

II. ELEMENTARY THEORETICAL CONSIDERATIONS

Let us first consider the description of the states of the Group IIIA-rare gas molecules without spin-orbit corrections. The valence $Ga(^2P) + Kr(^1S)$ separated atom limit gives rise to a $^2\Pi$ state and a $^2\Sigma^+$ state, the Rydberg $Ga(^2S) + Kr(^1S)$ limit gives rise to another $^2\Sigma^+$ state and the ionic $Ga^+(^1S) + Kr(^1S)$ limit gives rise to a $^1\Sigma^+$ state. We will label the states which arise from the valence limit the $1\,^2\Pi$ and $1\,^2\Sigma^+$ states, that from the Rydberg limit the $2\,^2\Sigma^+$ state and that from the ionic limit the $1\,^1\Sigma^+$ state.

The orbital diagrams for the $1\,^2\Pi$, $1\,^2\Sigma^+$, and $1\,^1\Sigma^+$ states of a Group IIIA-rare gas molecule are given in Fig. 1. From these diagrams it is evident that none of the resulting potential energy curves are expected to be chemically bound. In the ionic state, however, weak binding can result from the charge-induced dipole interaction of the Group IIIA ions and the rare gas atoms. In fact, this interaction might also be expected to give rise to a weak binding in the $2\,^2\Sigma^+$ state. Since the Rydberg orbital of the Group IIIA atom is diffuse, the approaching rare gas atom can easily polarize the Rydberg orbital out of the

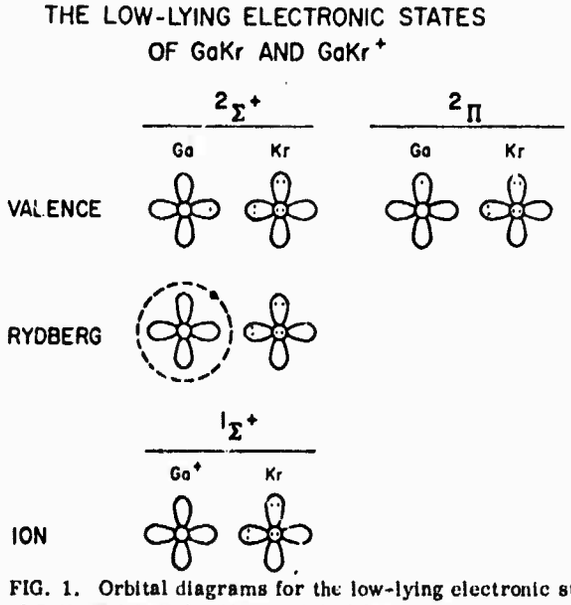

FIG. 1. Orbital diagrams for the low-lying electronic states of GaKr and GaKr$^+$. The two lobed figures represent 4*p* orbitals in the plane of the paper; the circle represents a 4*p* orbital perpendicular to the plane of the paper, the 5*s* Rydberg orbital is represented by a large dashed circle.

[a)] Research supported in part by the U. S. Department of Energy and by the Advanced Research Projects Agency under contract N00014-77-C-0102.

[b)] Present address: Theoretical Chemistry Group, Chemistry Division, Argonne National Laboratory, Argonne, Illinois 60439.

 0021-9606/78/6906-2672$01.00

interatomic region, thus partially unshielding the Group IIIA ionic core. The binding in the $2\,^2\Sigma^+$ state should, of course, be substantially less than that in the $1\,^1\Sigma^+$ state.

For the valence states the repulsiveness of the curves should be roughly proportional to the number of $p\sigma$ electrons since the overlap of the two atomic charge distributions is dominated by the overlap of the $p\sigma$ orbitals. Thus, the potential curve for the $1\,^2\Pi$ state with two $p\sigma$ electrons should be less repulsive than that for the $1\,^2\Sigma^+$ state with three $p\sigma$ electrons.

As we shall later see, at short internuclear separations the energies of the $1\,^2\Sigma^+$ and $2\,^2\Sigma^+$ states are nearly equal and there is a strong interaction between the two states. This mixing is strong in spite of the fact that one state is a valence state and the other a Rydberg state because the two zero-order configurations (see the next section) differ by only a single excitation.

A complete treatment of the electronic states of the Group IIIA-rare gas molecules must include the effects of spin-orbit coupling. Using the simple model developed in earlier papers for including the effects of spin-orbit coupling in diatomic molecules,[3] only the $1\,^2\Pi$ and $1\,^2\Sigma^+$ states are affected by the spin-orbit interaction, and the coupling arises solely from the spin-orbit interaction in the Group IIIA atom. For gallium the $^2P_{1/2}$–$^2P_{3/2}$ splitting is only 0.10 eV[4]; however, by thallium this splitting has increased to 0.97 eV.[4]

In a molecule only the z component of the total angular momentum,

$$\Omega = \Lambda + S_z \ ,$$

is a good quantum number. Thus, from the $\mathrm{Ga}(^2P_{1/2,3/2}) + \mathrm{Kr}(^1S_0)$ separated atom limits we obtain two $\Omega = 1/2$ states and one $\Omega = 3/2$ state (the *I* 1/2, *II* 1/2, and *I* 3/2 states), from the $\mathrm{Ga}(^2S_{1/2}) + \mathrm{Kr}(^1S_0)$ limit another $\Omega = 1/2$ state (the *III* 1/2 state), and from the $\mathrm{Ga}^*(^1S_0) + \mathrm{Kr}(^1S_0)$ limit an $\Omega = 0$ state (the 1 0 state). At large internuclear distances the *I* 3/2 and *II* 1/2 potential curves are degenerate and are separated from the *I* 1/2 (ground state) curves by the group IIIA $^2P_{3/2}$–$^2P_{1/2}$ splitting. As the distance decreases the $1\,^2\Pi$ and $1\,^2\Sigma^+$ curves rapidly separate, the separation increasing approximately exponentially. As a result at short distance the atomic spin-orbit coupling is nearly quenched and the *I* 1/2 and *II* 3/2 curves approximate the $1\,^2\Pi$ curve and the *II* 1/2 curve approximates the $1\,^2\Sigma^+$ curve. The potential curves of the $2\,^2\Sigma^+$ (*III* 1/2) and $1\,^1\Sigma^+$ (*I* 0) states are unaffected by the inclusion of spin-orbit coupling.

III. DETAILS OF THE CALCULATIONS

A. Basis sets

The calculations employed an atomic $(14s11p5d)$ primitive Gaussian basis set for both the gallium and krypton atoms.[5] The core orbitals ($1s, 2s, 3s, 2p, 3p$, and $3d$) were contracted to a single function while the valence orbitals ($4s$ and $4p$) were contracted to two functions using the general contraction method of Raffenetti[6] (see also Ref. 7). These atomic basis sets were augmented with a single set of $3d$ functions, $\zeta_{Ga} = 0.16$ and $\zeta_{Kr} = 0.35$, to describe molecular polarization effects. The values of these exponents were based on calculations on other excimer laser systems.[3,8]

Since the transition of interest involves the first Rydberg state of the gallium atom, the gallium basis set was augmented with two diffuse s functions, $\zeta_s = 0.026$ and 0.011, and a diffuse p function, $\zeta_p = 0.010$, to describe this state. The exponents of these functions were obtained from Hartree–Fock (HF) calculations on the ^2S and ^2P Rydberg states of the gallium atom.

The final basis sets thus consisted of a $(13s12p6d)$ primitive set contracted to $[7s5p2d]$ for gallium and a $(14s11p6d)$ primitive set contracted to $[5s4p2d]$ for krypton.

B. Calculations on the gallium atom

The *reference orbitals* for the configuration interaction (CI) calculations on the gallium atom were obtained from a Hartree–Fock (HF) calculation of the ^2P state of the atom with the configuration

$$^2P: \ \cdots 4s^2 4p \ . \tag{1}$$

(The $4p$ set includes all three cartesian components and all are equivalent.) The Rydberg $5s$ orbital was obtained from an IVO calculation[9] using the $4s^2$ core. In terms of these orbitals the *reference configurations* for the other states of interest are

$$^2S: \ \cdots 4s^2 5s \tag{2}$$

$$^1S: \ \cdots 4s^2 \ . \tag{3}$$

Both polarization CI (POL–CI)[10] and full CI calculations have been carried out on the above states of the gallium atom. The POL–CI calculations include all single and double excitations relative to configurations (1)–(3) with the restrictions that

(1) all core orbitals ($1s$–$3s$, $2p$–$3p$, and $3d$) remain doubly occupied and

(2a) no more than one electron occupy the Rydberg $5s$ *and* virtual orbitals (^2P and ^1S states) or

(2b) no more than one electron occupy the Rydberg $5s$ orbital *and* no more than one electron occupy the virtual orbitals (^2S state).

The POL–CI calculations involve 22 space and 33 space/spin configurations for the ^2P state, 27 space and 43 space/spin configurations for the ^2S state, and 15 space and 15 space/spin configurations for the ^1S state.[11] Note that the POL–CI wavefunction accounts for the $4s^2 - 4p^2$ near-degeneracy effect.

The less restrictive condition, (2b), for the ^2S state is necessary to obtain a comparable description of this state. Only by relaxing condition (2a) can configurations such as

$$\cdots [4p^2]5s$$

be included in the POL–CI wavefunction of the ^2S state. These configurations account for the first-order difference between the $4p$ orbital obtained from the calcula-

tions on the ^2P state and the p orbital needed to describe the angular correlation of the $4s^2$ pair ($4s$–$4p$ near degeneracy) and are quite important. Comparable configurations are automatically included in the POL–CI wavefunctions of the ^2P and ^1S states.

The full CI calculations include all excitattons (singie–triple) relative to the configurations (1)–(3) with only restriction (1) above. The full CI calculations include 157 space and 263 space/spin configurations for the ^2P state, 204 space and 306 space/spin configurations for the ^2S state, and 42 space and 4" space/spin configurations for the ^1S state.[11] Wiihin the frozen core approximation the accuracy of the results obtained from the full CI calculations is only limited by the completeness of the basis set.

C. Hartree–Fock calculations on GsKr

The *reference orbitals* for the POL–Cl calculations[10] on the GaKr molecule were obtained from an HF calculation on the $1\,^2\Sigma^+$ state with configuration[12]

$$\cdots 13\sigma^2 14\sigma^2 15\sigma^2 16\sigma 7\pi^4 \ . \tag{1a}$$

In the POL–CI calculations the core orbitals (12 σ orbitals, 12 π orbitals, and 4 δ orbitals) are always required to be doubly occupied and so it ts convenient to renumber the *valence orbitals* so that (1a) becomes

$$1\,^2\Sigma^+\!: \ 1\sigma^2 2\sigma^2 3\sigma^2 4\sigma 1\pi^4 \ . \tag{1b}$$

As $R\to\infty$ the above orbitals become

$1\sigma \to 4s_{Kr}$ $\quad 1\pi \to 4p\pi_{Kr}$

$2\sigma \to 4p\sigma_{Kr}$

$3\sigma \to 4s_{Ga}$

$4\sigma \to 4p\sigma_{Ga}$

The IVO method,[9] with a $1\sigma^2 2\sigma^2 3\sigma^2 1\pi^4$ core, was used to generate the *valence* 2π and *Rydberg* 5σ orbitals. As $R\to\infty$ these orbitals become the $4p\pi$ and $5s$ orbitals of the gallium atom. The virtual orbitals were also obtained from the IVO calculations.

In terms of the orbitals deftned in this way the *reference configurations* for the other states of tnterest are[12]

$$1\,^2\Pi\!: \quad 1\sigma^2 2\sigma^2 3\sigma^2 1\pi^4 2\pi \tag{2}$$

$$2\,^2\Sigma^+\!: \quad 1\sigma^2 2\sigma^2 3\sigma^2 5\sigma\, 1\pi^4 \tag{3}$$

$$1\,^1\Sigma^+\!: \quad 1\sigma^2 2\sigma^2 3\sigma^2 1\pi^4 \ . \tag{4}$$

D. Polarization configuration interaction calculstions on GaKr

Th: POL–CI calculations[10] on GaKr included all singie and double excitations relative to the reference configurations given above with the restrictions that

(1) all core orbitals remain doubly occupted and

(2a) no more than one electron occupy the Rydberg 5σ *and* virtual orbitals ($^2\Pi$ and $^1\Sigma^+$ states) or

(2b) no more than one electron occupy the Rydberg 5σ orbital *and* no more than one electron occupy the virtual orbitals ($^2\Sigma^+$ states).

For the $^2\Sigma^+$ states the calculations considered both states simultaneously. This procedure results in 556 space and 1565 space/spin configurations for the $^2\Pi$ states, 764 space and 2314 space/spin configurations for the $^2\Sigma^+$ states, and 368 space and 558 space/spin configurations for the $^1\Sigma^+$ state.

The less restrictive condition, (2b), is necessary for the $^2\Sigma^+$ states to allow for configurations such as

$$1\sigma^2 2\sigma^2[2\pi n\pi]5\sigma 1\pi^4 \ ,$$

which are important in the descrtption of the Rydberg $^2\Sigma^+$ state. As was the analogous case in the gallium atom, these configurations are necessary to allow for the inclusion of the $4s^2 - 4p^2$ near-degeneracy effect in the molecular wavefunction.

E. Inclusion of spin-orbit coupling in GaKr

As in our earlier calculations on excimer systems,[3,13] we have adopted a simple model[3] for tncluding the effects of sptn-orbit coupling on the calculated potential energy curves and wavefunctions. The experimental spin-orbit parameters for the open-shell atom, gallium in the present case, are used to determine the matrix elements of the spin orbit Hamiltonian, H_{so}, coupling the molecular states at $R=\infty$. These matrix elements are then assumed to be independent of R and are added to the diagonal matrix of the electronic energies

$$H^{\Omega}(R) = \delta_{ij} E_i(R) + H_{so} \ . \tag{5}$$

The energies and wavefunctions with spin-orbit corrections are obtained by diagonalizing $H^{\Omega}(R)$. Thls procedure is reasonable only so long as (1) the molecular states retain the identity of the atomic states from which they arise and (2) the atomic contributions to the molecular spin-orbtt interactions are dominant.

For GaKr the spin-orbit interaction affects only those states which arise from the $Ga(^2P) + Kr(^1S)$ limit. The Hamiltonian matrix for the $\Omega = 1/2$ states artsing from this limit is

$$H^{\Omega=1/2} = \begin{bmatrix} E(1\,^2\Sigma^+) & \sqrt{2}\,\lambda_{Ga} \\ \sqrt{2}\lambda_{Ga} & E(1\,^2\Pi) - \lambda_{Ga} \end{bmatrix} \tag{6a}$$

and for the $\Omega = 3/2$ state is

$$H^{\Omega=3/2} = E(1\,^2\Pi) + \lambda_{Ga} \ . \tag{6b}$$

In (6) λ_{Ga} is one third of the $^2P_{3/2}$–$^2P_{1/2}$ splitting in the gallium atom. The energies of the $2\,^2\Sigma^+$ and $1\,^1\Sigma^+$ states of GaKr are unaffected by the incluston of sptn-orbit coupiing. The wavefunctions for the states obtatned by diagonalizing (6) may be written in the form

$$|I\,1/2\rangle = \cos\theta\,|1\,^2\Pi_{,}\beta\rangle + \sin\theta\,|1\,^2\Sigma^+\alpha\rangle \tag{7a}$$

$$|II\,1/2\rangle = -\sin\theta\,|1\,^2\Pi_{,}\beta\rangle + \cos\theta\,|1\,^2\Sigma^+\alpha\rangle \tag{7b}$$

$$|I\,3/2\rangle = |1\,^2\Pi_{,}\alpha\rangle \ , \tag{7c}$$

where θ is the spin rotation angle. The wavefunctions for the $|III\,1/2\rangle$ and $|I0\rangle$ states are

$$|III\,1/2\rangle = |2\,^2\Sigma^+\alpha\rangle \tag{7d}$$

$$|I0\rangle = |1\,^1\Sigma^+\rangle \ . \tag{7e}$$

TABLE I. Calculations on the ^2P, ^2S, and ^1S (ion) states of Ga and the ^1S state of krypton. For Ga the experimental results have been corrected for spin-orbit effects (see the text). Units are as indicated.

Atom state	Ga ^2P	Ga(Ga$^+$) ^2S	Ga(Ga$^+$) ^1S	Kr ^1S
Total energies (hartree)[a]				
POL–CI	0.22523	0.12130	0.01912	0.97377[b]
Full CI	0.23484	0.12750	0.02305	···
Excitation energies (eV)				
POL–CI	0.00	2.83	5.61	···
Full CI	0.00	2.92	5.76	···
Expt'l[c]	0.000	3.005	5.930	···
Transition moment (ea_0)				
POL–CI	···	−1.298[d]	···	···
Lifetimes (nsec)				
POL–CI	···	8.2[e]	···	···
Expt'l	···	6.8[f]	···	···

[a]For Ga the energies are relative to −1923 hartree; for Kr the energies are relative to −2751 hartree.
[b]For Kr the POL–CI wavefunction is equivalent to the HF wavefunction.
[c]Reference 4.
[d]This is the matrix element $1/3|\langle {}^2S|x|{}^2P_x\rangle + \langle {}^2S|y|{}^2P_y\rangle + \langle {}^2S|z|{}^2P_z\rangle|$.
[e]Using the experimental excitation energy we obtain 6.9 nsec.
[f]Reference 14.

With the definitions (7) the dipole transition moments coupling the $III\,1/2$ state with all of the lower states are

$$\mu_z(III\,1/2 - I\,1/2) = \sin\theta\,\langle 2\,{}^2\Sigma^+|z|1\,{}^2\Sigma^+\rangle \quad (8a)$$

$$\mu_x(III\,1/2 - I\,1/2) = \cos\theta\,\langle 2\,{}^2\Sigma^+|x|1\,{}^2\Pi_x\rangle/\sqrt{2} \quad (8b)$$

$$\mu_z(III\,1/2 - II\,1/2) = -\cos\theta\,\langle 2\,{}^2\Sigma^+|z|1\,{}^2\Sigma^+\rangle \quad (9a)$$

$$\mu_x(III\,1/2 - II\,1/2) = \sin\theta\,\langle 2\,{}^2\Sigma^+|x|1\,{}^2\Pi_x\rangle/\sqrt{2} \quad (9b)$$

$$\mu_x(III\,1/2 - I\,3/2) = -\langle 2\,{}^2\Sigma^+|x|1\,{}^2\Pi_x\rangle/\sqrt{2}\ . \quad (10)$$

Since the $\langle 2\,{}^2\Sigma^+|x|1\,{}^2\Pi_x\rangle$ transition moment is expected to be comparable in magnitude to the $\langle 2\,{}^2\Sigma^+|z|1\,{}^2\Sigma^+\rangle$ moment (at $R=\infty$ they are identical), it is clear from (8) and (9) that the transitions from the $III\,1/2$ state of the $I\,1/2$ and $II\,1/2$ states can have both large parallel and perpendicular components.

IV. RESULTS FOR Ga, GaKr, AND GaKr$^+$

A. Electronic states of Ga, without spin-orbit corrections

The results of the calculations on the Ga atom are summarized in Table I. The computed ^2S–^2P excitation energy is 2.83 eV (POL–CI) and 2.92 eV (full CI). Averaging the multiplet energies for the $^2P_{1/2}$ and $^2P_{3/2}$ states of gallium from Moore,[4] the experimental ^2S–^2P splitting is calculated to be 3.005 eV, just 0.08–0.17 eV larger than the computed spacing. The errors in the calculated ionization potentials, 5.61 eV (POL–CI) and 5.76 eV (full CI), are somewhat larger, being 0.32 and 0.17 eV, respectively.

The lifetime of the ^2S state of gallium has been determined by Norton and Gallagher[14] to be 6.8 ± 0.3 nsec. For the model used here the lifetime of the ^2S state is independent of the spin-orbit corrections. From the POL–CI wavefunctions we calculate a lifetime of 8.2 nsec for the ^2S state (6.9 nsec, if the experimental excitation energy is used instead of the calculated excitation energy).

B. Electronic states of GaKr and GaKr$^+$, without spin-orbit corrections

The energies of the $1\,{}^2\Pi$, $1,2\,{}^2\Sigma^+$, and $1\,{}^1\Sigma^+$ states of GaKr and GaKr$^+$ obtained from the POL–CI calculations are listed in Table II and the resulting potential energy curves are plotted in Fig. 2. As is usual in such calculations,[3,8,13] the energies of the $1\,{}^2\Pi$ and $1\,{}^2\Sigma^+$ states, both of which arise from the ^2P limit, are not exactly equal at $R = 15.0\,a_0$ (the largest value of R considered). The difference, 0.00114 hartree (0.031 eV), is attributable to the inequivalence of the $4p\sigma$ and $4p\pi$ orbitals and to core polarization effects (the core orbitals were obtained from HF calculations on the $1\,{}^2\Sigma^+$ state which does not have the full rotational symmetry of the atom). In the plots the asymptotic energies of the states have been adjusted to give the experimental atomic energy splittings.

In line with the discussion in Sec. II, the potential energy curve for the $1\,{}^2\Pi$ state is found to be less repulsive than that of the $1\,{}^2\Sigma^+$ state, thus making the $1\,{}^2\Pi$ state the ground state of the system. In fact, we find that the $1\,{}^2\Pi$ curve is slightly bound, $D_e \sim 0.04$ eV (see Table III). Although spurious minima have been found in previous calculations on excimer systems[8,13] and attributed to basis set limitations, the well in the $1\,{}^2\Pi$ curve is substantially larger than has been observed heretofore. We thus suspect that the minimum in the $1\,{}^2\Pi$ curve is not just a result of calculational limitations. The depth of the well in the real $1\,{}^2\Pi$ curve is, of course, expected to be significantly larger than that calculated here since the POL–CI method is not designed to account for the attractive van der Waals' interaction.

As predicted in Sec. II both the $2\,{}^2\Sigma^+$ and $1\,{}^1\Sigma^+$ curves

TABLE II. Energies obtained from the POL–CI calculations on the low-lying electronic states of GaKr and GaKr$^+$. Distances are in bohr; energies are in hartree. Energies are relative to −4674 hartree.

R	GaKr $1\,{}^2\Pi$	GaKr $1\,{}^2\Sigma^+$	GaKr $2\,{}^2\Sigma^+$	GaKr$^+$ $1\,{}^1\Sigma^+$
3.75	−1.02539	−0.96866	−0.93379	−0.85625
4.00	−1.07933	−1.01870	−0.99238	−0.90683
4.50	−1.14810	−1.08688	−1.06410	−0.96758
5.00	−1.17924	−1.13516	−1.08855	−0.99287
5.50	−1.19225	−1.16324	−1.09545	−1.00070
6.00	−1.19772	−1.17938	−1.09677	−1.00202
6.50	−1.19984	−1.18865	−1.09631	−1.00107
7.00	−1.20045	−1.19396	−1.09545	−0.99950
8.00	−1.20020	−1.19865	−1.09420	−0.99670
10.00	−1.19933	−1.20029	−1.09406	−0.99402
15.00	−1.19878	−1.20012	−1.09502	−0.99304

THE LOW-LYING STATES OF GaKr AND GaKr$^+$

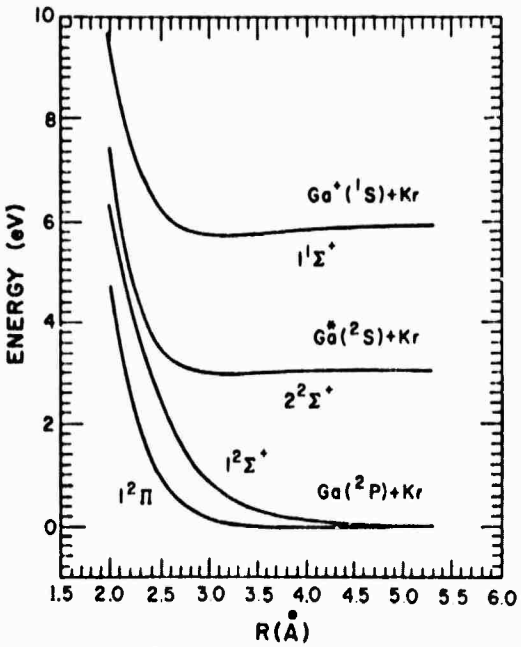

FIG. 2. Calculated potential energy curves for the states of GaKr and GaKr$^+$ arising from the Ga(^2P, ^2S) + Kr(^1S) and Ga$^+$(^1S) + Kr(^1S) separated atom limits. The curves have been uniformly shifted to correct for the errors in the gallium atom excitation energies.

are found to be bound with calculated dissociation energies of 0.047 and 0.24 eV, respectively. Again, inclusion of the attractive van der Waals' interaction would be expected to significantly increase the calculated well depths. There is a slight hump in the calculated potential curve of the $2^2\Sigma^+$ state, ~0.026 eV, since the long-range interaction of the excited Ga and Kr atoms is repulsive. This hump could, however, disappear when the van der Waals' attraction is added to the calculated curve.

The dipole transition moments radiatively coupling the states of GaKr are given in Table IV and plotted in Fig. 3. At $R=\infty$ the transition moment coupling the $1^2\Pi$ and $1^2\Sigma^+$ states is identically zero and those coupling the ($1^2\Pi$, $1^2\Sigma^+$) states with the $2^2\Sigma^+$ state are approximately equal to the ^2S–^2P atomic transition moment (after properly accounting for differences in degeneracy factors). As R decreases rather minor changes occur until $R\sim 2.5$ Å. For $R<2.5$ Å substantial changes are noted in all of the transition moments, although the change in the $2^2\Sigma^+$–$1^2\Pi$ moment is less dramatic than for the $2^2\Sigma^+$–$1^2\Sigma^+$ and $1^2\Sigma^+$–$1^2\Pi$ moments. The erratic behavior of the transition moments for $R<2.5$ Å is one manifestation of the strong interaction of the $1^2\Sigma^+$ and $2^2\Sigma^+$ states at short R.

TABLE III. Spectroscopic constants for the bound states of ^{69}Ga^{84}Kr and ^{69}Ga^{84}Kr$^+$. Units are as indicated.

	GaKr		GaKr$^+$
	$1^2\Pi$	$2^2\Sigma^+$	$1^2\Sigma^+$
T_e, eV	0.00	2.82	5.40
R_e, Å	3.78	3.17	3.14
D_e, eV	0.041	0.047	0.24
ω_e, cm^{-1}	36	66	83
B_e	0.0312	0.0442	0.0452

TABLE IV. Dipole transition moments coupling the low-lying states of GaKr obtained from the POL–CI calculations.

R	$1^2\Sigma^+$–$1^2\Pi^a$	$2^2\Sigma^+$–$1^2\Pi^a$	$2^2\Sigma^+$–$1^2\Sigma^+$
3.75	−0.9037	−0.7877	0.4095
4.00	−0.8462	−0.8680	−0.3055
4.50	−0.1365	−1.2090	−2.0676
5.00	0.0992	−1.2349	−1.4402
5.50	0.1257	−1.2469	−1.2456
6.00	0.1166	−1.2554	−1.1893
6.50	0.0984	−1.2619	−1.1800
7.00	0.0789	−1.2677	−1.1902
8.00	0.0476	−1.2777	−1.2310
10.00	0.0163	−1.2898	−1.2976
15.00	0.0018	−1.2917	−1.3101

[a]The matrix element given is $\langle n^2\Sigma^+|x|1^2\Pi_x\rangle$.

Although, as noted above, substantial changes are found in the transition moments for $R<2.5$ Å, such behavior can be expected to have little effect on the observable properties of the system. At $R=2.5$ Å the energy of the $2^2\Sigma^+$ state is >0.5 eV above its asymptote so that the region $R<2.5$ Å would be thermally inacessible.

DIPOLE TRANSITION MOMENTS AMONG THE LOW-LYING STATES OF GaKr

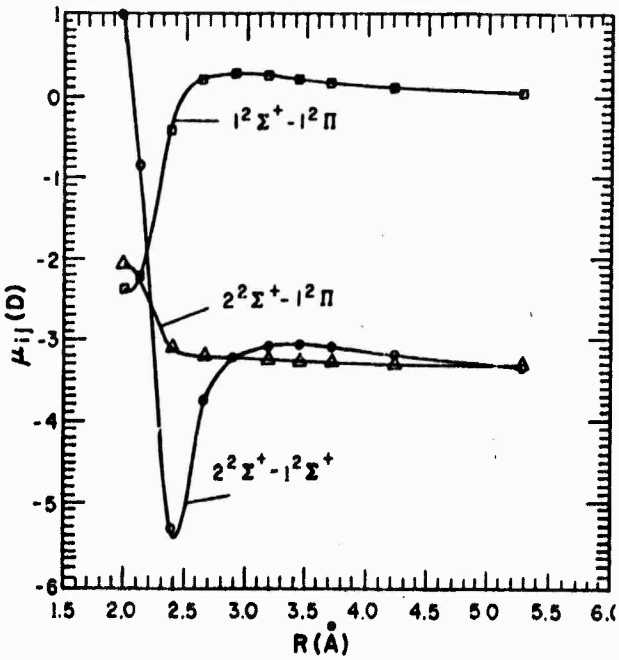

FIG. 3. Calculated dipole transition moments for the $1^2\Sigma^+$–$1^2\Pi$, $2^2\Sigma^+$–$1^2\Pi$, and $2^2\Sigma^+$–$1^2\Sigma^+$ transitions in GaKr.

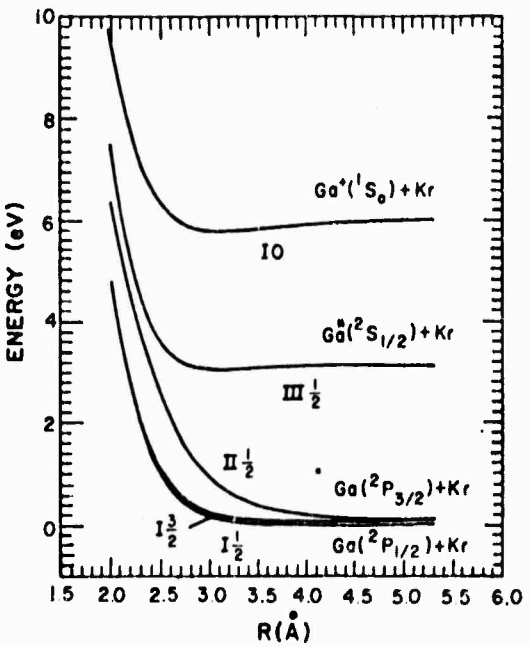

FIG. 4. Calculated potential energy curves for the states of GaKr and GaKr$^+$ arising from the $Ga(^2P_{1/2,3/2}, {}^2S_{1/2}) + Kr(^1S_0)$ and $Ga^+(^1S_0) + Kr(^1S_0)$ separated atom limits. The curves have been uniformly shifted to correct for the errors in the gallium excitation energies.

C. Electronic states of GaKr and GaKr$^+$, with spin-orbit corrections

The energies of the states of GaKr and GaKr$^+$ with spin-orbit corrections are given in Table V and the resulting potential energy curves are plotted in Fig. 4. In calculating the spin-orbit corrected energies we shifted the $1\,^2\Pi$ energies to agree with the $1\,^2\Sigma^+$ energy at the largest value of R considered ($R = 15.0a_0$). Again, in plotting the potential energy curves, the asymptotic energies of the states have been adjusted to give the correct atomic energy splittings.

As predicted in Sec. II, at short R the curves for the

TABLE V. Calculated energies of the I 1/2, II 1/2, and I 3/2 states of GaKr with spin-orbit corrections. Distances are in bohr; energies are in hartree. Energies are relative to the energy of the $1\,^2\Sigma^+$ state at $R = 15\ a_0$.

R	I 1/2	I 3/2	II 1/2
3.75	0.17228	0.17484	0.23152
4.00	0.11835	0.12091	0.18147
4.50	0.04957	0.05213	0.11329
5.00	0.01841	0.02099	0.06502
5.50	0.00538	0.00799	0.03698
6.00	−0.00015	0.00252	0.02089
6.50	−0.00234	0.00040	0.01170
7.00	−0.00307	−0.00022	0.00650
8.00	−0.00316	0.00003	0.00215
10.00	−0.00280	0.00090	0.00103
15.00	−0.00251	0.00126	0.00126

TABLE VI. Calculated dipole transition moments coupling the III 1/2 and I 1/2, II 1/2 and I 3/2 states of GaKr with spin-orbit corrections. Distances are in bohr; moments are in atomic units.

	III 1/2–I 1/2		III 1/2–II 1/2		III 1/2–I 3/2
R	z	(x,y)	z	(x,y)	(x,y)
4.00	−0.0086	0.6135	−0.3054	−0.0173	−0.6138
4.50	−0.0576	0.8545	−2.0667	−0.0238	−0.8549
5.00	−0.0549	0.8726	−1.4392	−0.0333	−0.8732
5.50	−0.0701	0.8803	−1.2437	−0.0496	−0.8817
6.00	−0.1007	0.8845	−1.1850	−0.0752	−0.8877
6.50	−0.1504	0.8850	−1.1704	−0.1138	−0.8923
7.00	−0.2249	0.8803	−1.1688	−0.1694	−0.8964
8.00	−0.4405	0.8436	−1.1495	−0.3233	−0.9035
10.00	−0.7254	0.7562	−1.0759	−0.5098	−0.9120
15.00	−0.7564	0.7457	−1.0697	−0.5273	−0.9134

$I$1/2 and $I$3/2 states become nearly degenerate and just represent the curves for the two spin-orbit components of the $1\,^2\Pi$ state. Also, at short R the $II$1/2 curve closely approximates the curve for the $1\,^2\Sigma^+$ state. The potential energy curves for the $2\,^2\Sigma^+$ ($III$1/2) and $1\,^1\Sigma^+$(I0) states are unchanged by the inclusion of spin-orbit corrections.

The dipole transition moments radiatively coupling the states of GaKr with spin-orbit corrections are given in Table VI and are plotted in Fig. 5. It should be noted that both the z component of the $III$1/2–$I$1/2 transition and the x component of the $III$1/2–$II$1/2 transition are now found to vary significantly even for $R > 2.5$ Å. This is due to the changing nature of the $I$1/2 and $II$1/2 states

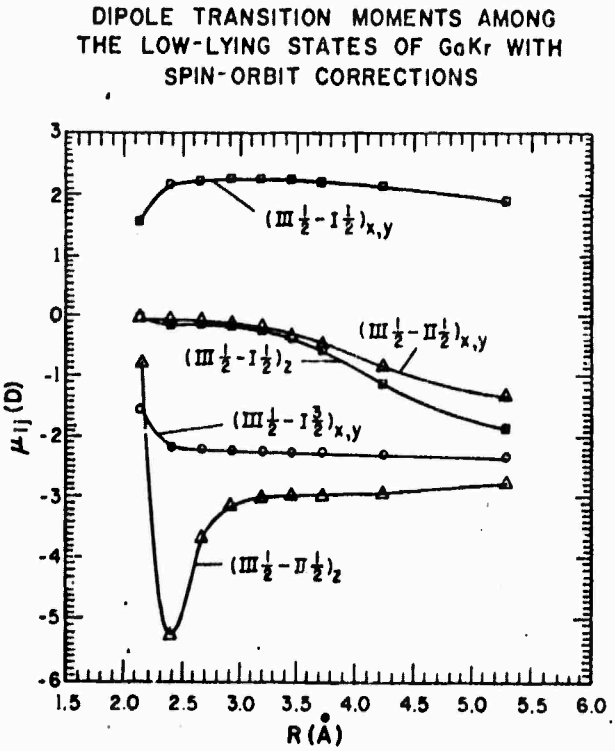

FIG. 5. Calculated dipole transition moments for the III 1/2–I 1/2, III 1/2–I 3/2, and III 1/2–II 1/2 transitions in GaKr.

TABLE VII. Excitation energies and ionization potentials for the Ga, In, and Tl atoms, in eV. Taken from Ref. 4.

	Group IIIA atoms		
State	Ga	In	Tl
$^2P_{1/2}$	0.000	0.000	0.000
$^2P_{3/2}$	0.102	0.274	0.966
$^2S_{1/2}$	3.073	3.022	3.282
$^1S_0$	5.998	5.786	6.108

as the atomic spin-orbit coupling is quenched by molecular formation.

V. EXTRAPOLATION TO InKr AND TlKr

To provide information on the InKr and TlKr molecules, the latter being the most experimentally accessible of the Group IIIA-krypton molecules, the potential curves for InKr and TlKr have been estimated from the GaKr curves. The excitation energies and ionization potentials for the series Ga, In, and Tl are given in Table VII. As can be seen, this series does not form a steady progression: In has a lower ionization potential and excitation energies than Ga, as expected, but Tl has a higher ionization potential and excitation energies. This anomalous behavior in Tl is due in part to the filling of the 4*f* shell ("lanthanide contraction") and to the larger spin-orbit interactions.[15] These effects are only partially accounted for in the present models.

To simulate InKr and TlKr, the experimental spin-orbit parameters for In and Tl, see Table VII, were used to couple the curves calculated for GaKr. The potential energy curves for InKr and TlKr obtained in this way are expected to be qualitatively correct; the curves are plotted in Figs. 6 and 7. As before, the plotted

THE LOW-LYING STATES OF InKr AND InKr$^+$ WITH SPIN-ORBIT CORRECTIONS

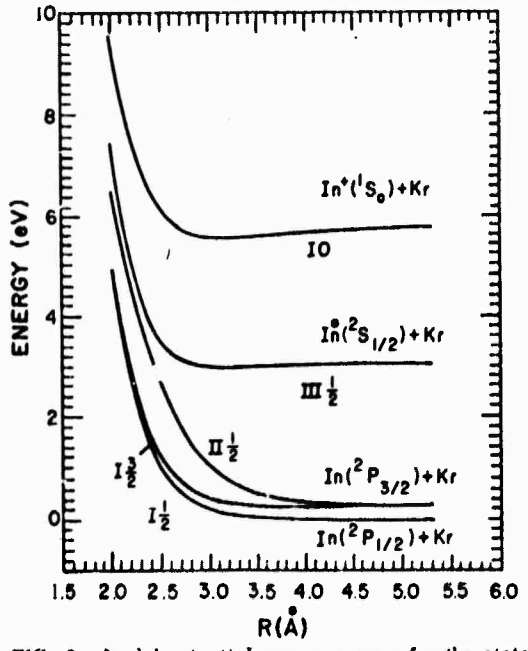

FIG. 6. Model potential energy curves for the states of InKr and InKr$^+$ arising from the In($^2P_{1/2,3/2}$, $^2S_{1/2}$) + Kr($^1S_0$) and In$^+$($^1S_0$) + Kr($^1S_0$) separated atom limits, see the text.

THE LOW-LYING STATES OF TlKr AND TlKr$^+$ WITH SPIN-ORBIT CORRECTIONS

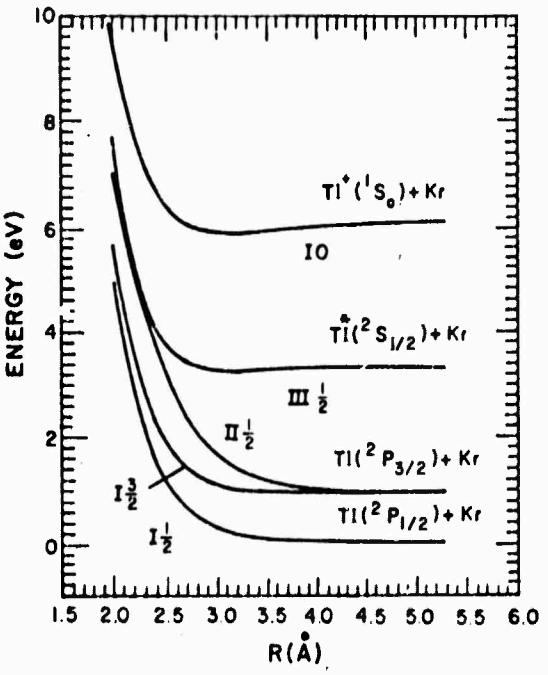

FIG. 7. Model potential energy curves for the states of TlKr and TlKr$^+$ arising from the Tl($^2P_{1/2,3/2}$, $^2S_{1/2}$) + Kr($^1S_0$) and In$^+$($^1S_0$) + Kr($^1S_0$) separated atom limits, see the text.

DIPOLE TRANSITION MOMENTS CONNECTING THE LOW-LYING STATES OF TlKr WITH SPIN-ORBIT CORRECTIONS

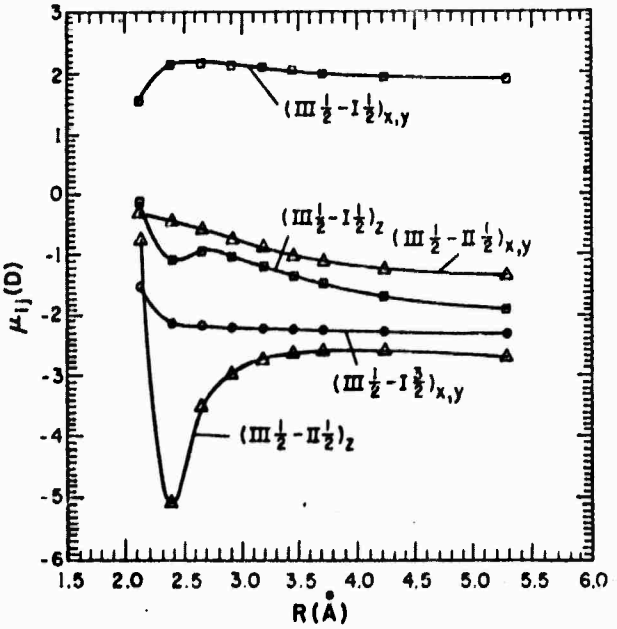

FIG. 8. Model dipole transition moments for the *III* 1/2–*I* 1/2, *III* 1/2–*I* 3/2, and *III* 1/2–*II* 1/2 transitions in TlKr.

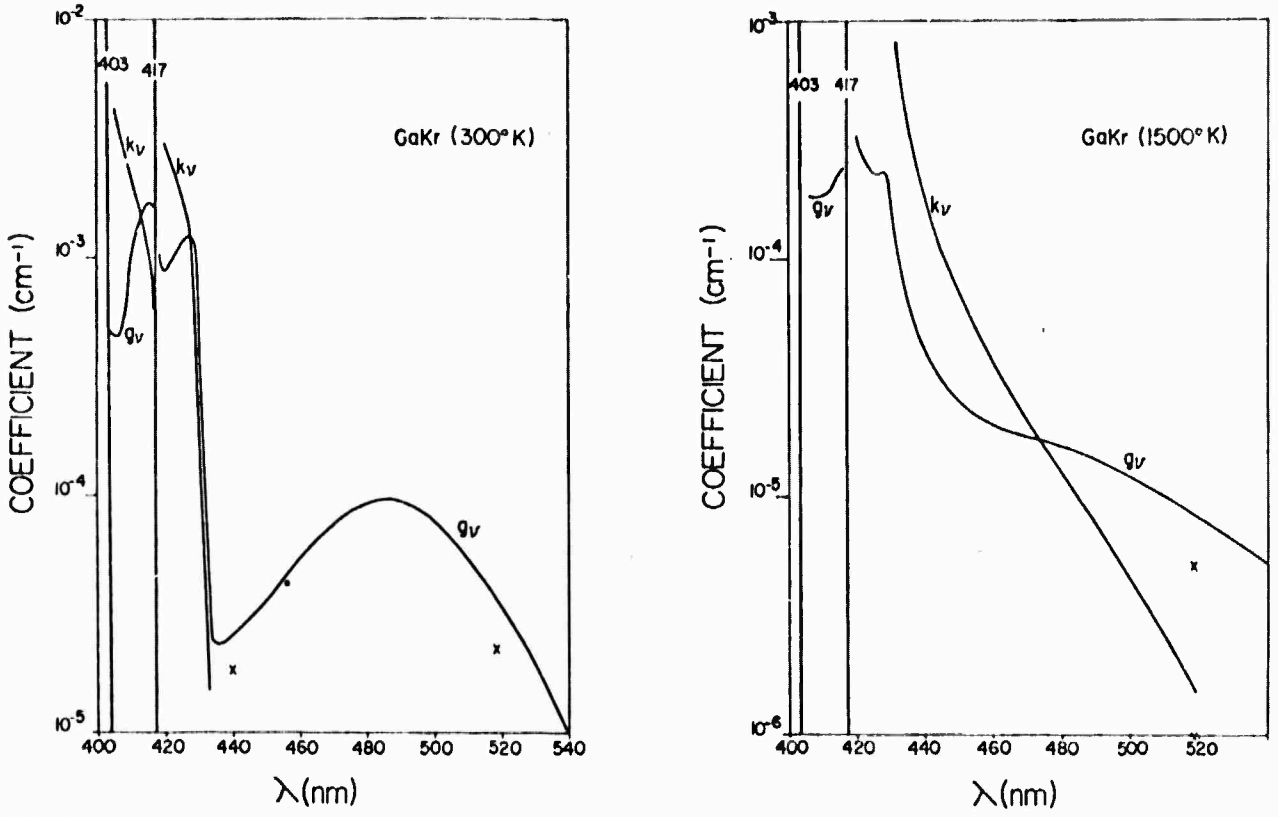

FIG. 9. Calculated absorption, $K_\nu(T)$, and stimulated emission, $g_\nu(T)$, coefficients for GaKr at $T = 300$ and 1500 °K.

curves have been shifted to give the correct atomic excitation energies. The effect of the increasing spin-orbit interaction in the sequence Ga < In < Tl is evident in Figs. 4, 6, and 7.

Using the transition moments obtained from the calculations on GaKr and the wavefunctions obtained from the TlKr simulation, the transition moments of TlKr have been estimated. The moments so obtained are plotted in Fig. 8.

VI. ABSORPTION AND STIMULATED EMISSION COEFFICIENTS FOR GaKr, InKr, AND TlKr

The interest in the Group IIIA-rare gas systems arises from the possibility of their use as visible laser systems. In order to judge their usefulness as lasers it is convenient to calculate the pure absorption, $K_\nu(T)$, and stimulated emission, $g_\nu(T)$, coefficients for the perturbed atomic transitions. Obtaining quantum mechanical results for these quantities would require a complex calculation which is not justified by the extrapolations used to obtain the InKr and TlKr curves. Consequently, we have used instead the method of Gallagher and coworkers,[16] which is based on the classical Franck–Condon principle. In this approximation

$$g_\nu(T)_J = [M^*][X](\lambda^2/8\pi)A_0(J)(\lambda/\lambda_0)I'_J(\nu T)$$

$$K_\nu(T) = [M][X](g^*/g)g_\nu(T)_J \exp[h(\nu-\nu_0)/kT]$$

and

$$I'_J(\nu, T) = 4\pi R(\nu)^2\left(\frac{\nu}{\nu_0}\right)^4 \frac{1}{d\nu/dR(\nu)} \frac{D[R(\nu)]}{D(\infty)} \frac{g_m}{g_A} \times \exp\{-V^*[R(\nu)]/kT\} .$$

In these equations, J refers to the bands associated with the $^2S_{1/2}$–^2P_J transition, ν_0 and λ_0 are the frequency and wavelength of the atomic transition with a transition rate of $A_0(J)$, $g^* = 2$ for the $^2S_{1/2}$ state and $g = 2J+1$ for the ^2P_J states, $D(R)$ is the transition dipole moment at R, g_m and g_A are the statistical weights of the excited molecular and parent atomic state, and $V^*(R)$ is the excited state potential curve relative to the energy of the excited atomic state. [M], [M*], and [X] are the concentrations of ground and excited metal atoms and of rare gas atoms at the temperature T.

In order to obtain $g_\nu(T)$ and $K_\nu(T)$, the calculated curves were first fit with cubic splines. The spline fit was then used to calculate $d\nu/dR$, and these quantities, along with the atomic transition rates,[14] were used to calculate the absorption and stimulated emission coefficients for pressure and excitation conditions relevant to the experimental studies. We have calculated the coefficients for two different types of conditions. The high temperature results correspond to the case where the concentration of the metal is obtained from the vapor pressure of the metal itself, while the low temperature results correspond to obtaining the required concentration of the metal from vaporization of MI_3. This latter condition has been suggested by Gallagher[2] as a possible means of obtaining high concentrations of the metal at low temperatures. In both cases the densities used are

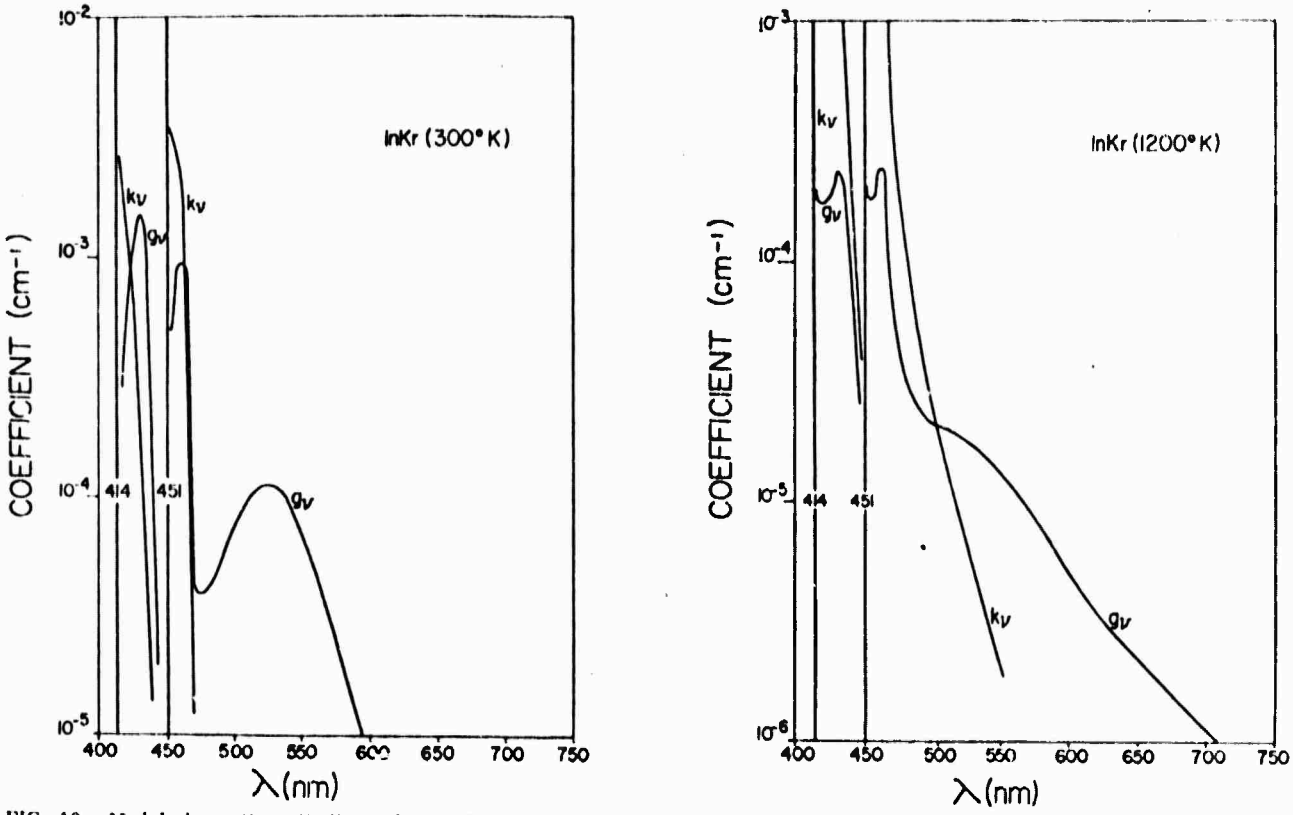

FIG. 10. Model absorption, $K_\nu(T)$, and stimulated emission, $g_\nu(T)$, coefficients for InKr at $T = 300$ and 1200 °K.

$10^{20}/\text{cm}^3$ for [Kr], $10^{16}/\text{cm}^3 = 3[\text{M}(^2P_{1/2})] = 1.5[\text{M}(^2P_{3/2})]$, and $2\times10^{14}/\text{cm}^3$ for $[\text{M}(^2S_{1/2})]$. Since the blue wings of the $^2S_{1/2}$–$^2P_{1/2,3/2}$ bands are due to transitions occurring at large R, where our curves are not expected to be especially accurate, we have not calculated g_ν and K_ν in these regions.

The resulting absorption and stimulated emission coefficients for GaKr, InKr, and TlKr are given in Figs.

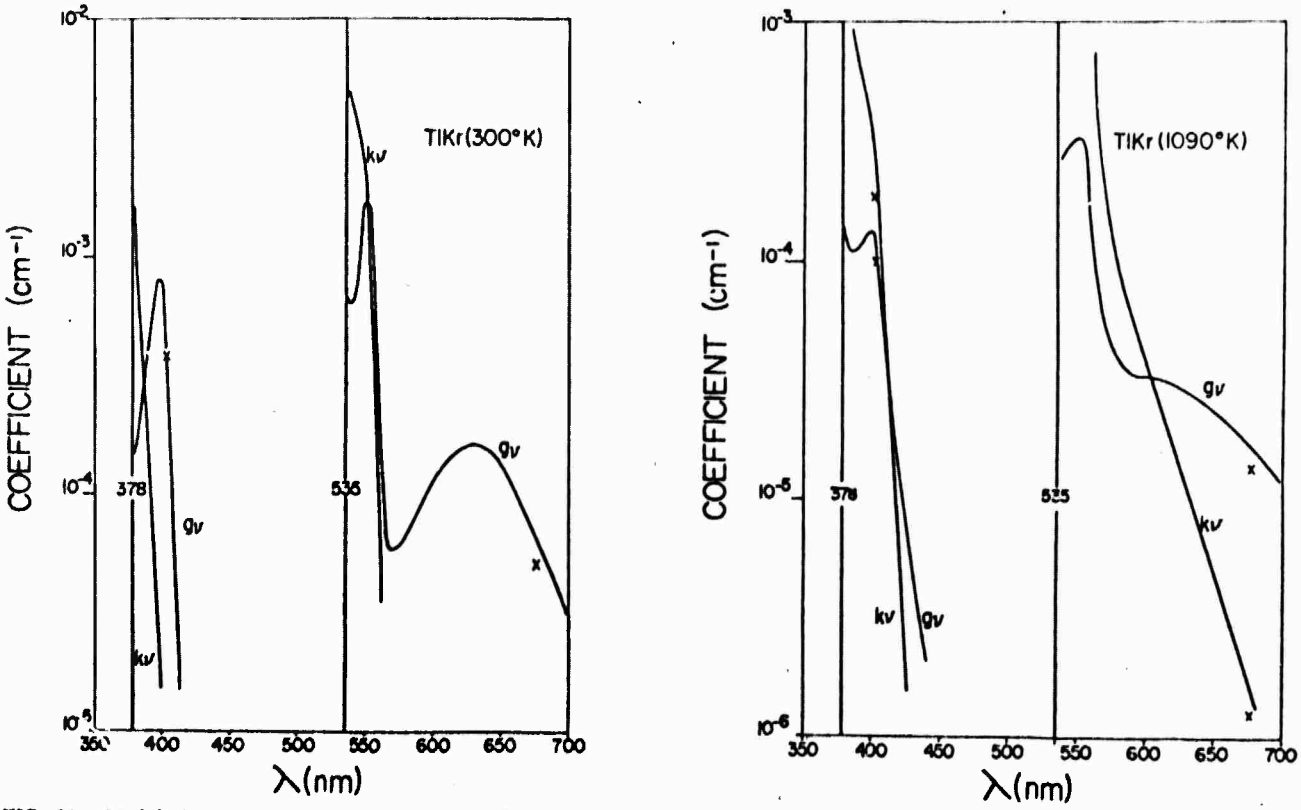

FIG. 11. Model absorption, $K_\nu(T)$, and stimulated emission, $g_\nu(T)$, coefficients for TlKr at $T = 300$ and 1090 °K.

9–11. In these figures the solid lines are the total coefficients calculated by assuming that the transition moment, $D(R)$, is a constant. The X's are the coefficients obtained by using the spatially averaged values of $D(R)$ calculated from Table VI and the appropriate spin-orbit parameters. For GaKr at 1500 °K (Fig. 10) and for $403.4 < \lambda < 417.3$ nm, $K_\nu > 10^{-3}$ cm^{-1}. The dip in g_ν close to the line center is due to the positive value of $V^*(R \sim 8a_0) - V^*(R = \infty)$.

The gain coefficient, which is approximately equal to $g_\nu - K_\nu$ can be estimated from these curves. For the frequencies at which gain occurs, the use of $D(R)$ decreases g_ν, K_ν, and the gain by 30–40% for GaKr and by 9–15% for TlKr. For TlKr the errors introduced by the extrapolation procedure are likely to be larger than those produced by using $D(\infty)$ rather than $D(R)$. The maximum gain occurs approximately at the minimum in the $III\,1/2$ curve. Because g_ν depends exponentially on V^*, changes in the well depth of the excited state would have a significant effect on g_ν. If the well depth were larger for TlKr, as Gallagher and co-workers predict,[1] g_ν and the gain would be larger. Likewise, since the excited state in TlXe is predicted[1] to be more bound than in TlKr, the gain should be larger for TlXe than for TlKr.

[1]B. Cheron, R. Scheps, and A. Gallagher, J. Chem. Phys. 65, 326 (1976).
[2]A. Gallagher, private communication.
[3]P. J. Hay, T. H. Dunning, Jr. and R. C. Raffenetti, J. Chem. Phys. 65, 2679 (1976).
[4]C. E. Moore, *Atomic Energy Levels*, National Bureau of Standards, Circular No. 467, Vols. I–III. (U.S. GPO, Washington, D. C., 1949).
[5]T. H. Dunning, Jr., J. Chem. Phys. 66, 1382 (1977).
[6]R. C. Raffenetti, J. Chem. Phys. 58, 4452 (1973).
[7]T. H. Dunning, Jr. and P. J. Hay in *Methods of Electronic Structure Theory*, edited by H. F. Schaefer, III (Plenum, New York, 1977), Chap. 1.
[8]T. H. Dunning, Jr. and P. J. Hay, J. Chem. Phys. 66, 3767 (1977).
[9]W. J. Hunt and W. A. Goddard, III, Chem. Phys. Lett. 3, 414 (1969).
[10]P. J. Hay and T. H. Dunning, Jr., J. Chem. Phys. 64, 5077 (1976); T. H. Dunning, Jr., J. Chem. Phys. 65, 3854 (1976). The POL–CI wavefunction is closely related to the first-order wavefunction of Schaefer, Harris, and co-workers, see, e.g., H. F. Schaefer, III, R. A. Klemm, and F. E. Harris, J. Chem. Phys. 51, 4643 (1969).
[11]The CI program cannot make full use of the atomic or diatomic symmetry. The numbers of configurations quoted in the text are for C_{2v} symmetry.
[12]For the states of interest here the generalized valence bond wavefunctions would also include the s–p near-degeneracy configurations. As noted in the text these configurations are included in the POL–CI wavefunctions.
[13]P. J. Hay and T. H. Dunning, Jr., J. Chem. Phys. 66, 1306 (1977).
[14]M. Norton and A. Gallagher, Phys. Rev. A 3, 915 (1971).
[15]P. Bagus, Y. S. Lee, and K. S. Pitzer, Chem. Phys. Lett. 33, 408 (1975).
[16]R. Scheps, Ch. Ottinger, G. York, and A. Gallagher, J. Chem. Phys. 63, 2581 (1975).

Appendix B

```
;  <WATTS>0000.24;10    WED 15-NOV-78 8:55AM

operator sinh,cosh,re,ef,ra,ab,ra,dr;
array ee(3),ff(3),bb(3);
for all x let df(sinh(x),x) = cosh(x);
for all x let df(cosh(x),x) = sinh(x);
let ee(1)=ex,ee(2)=ey,ee(3)=ez,ff(1)=fx,ff(2)=fy,ff(3)=fz,bb(1)=bx,bb(2)=by,BB(3)=BZ
let df(re(ee,ff),ex)  =  ef(ex,fx)/re(ee,ff);
let df(re(ee,ff),ey)  =  ef(ey,fy)/re(ee,ff);
let df(re(ee,ff),ez)  =  ef(ez,fz)/re(ee,ff);
let df(re(ee,ff),fx)  = -ef(ex,fx)/re(ee,ff);
let df(re(ee,ff),fy)  = -ef(ey,fy)/re(ee,ff);
let df(re(ee,ff),fz)  = -ef(ez,fz)/re(ee,ff);
let df(re(ee,ff),bx)  = 0;
let df(re(ee,ff),by)  = 0;
let df(re(ee,ff),bz)  = 0;
let df(ef(ex,fx),ex)  =  1;
let df(ef(ex,fx),fx)  = -1;
let df(ef(ey,fy),ey)  =  1;
let df(ef(ey,fy),fy)  = -1;
let df(ef(ez,fz),ez)  =  1;
let df(ef(ez,fz),fz)  = -1;
for all x,y let df(ef(x,y),bx) = 0;
for all x,y let df(ef(x,y),by) = 0;
for all x,y let df(ef(x,y),bz) = 0;
let df(ra(ee,ff,bb),ex)  =  (a/c)*ab(ex,fx,bx)/ra(ee,ff,bb);
let df(ra(ee,ff,bb),ey)  =  (a/c)*ab(ey,fy,by)/ra(ee,ff,bb);
let df(ra(ee,ff,bb),ez)  =  (a/c)*ab(ez,fz,bz)/ra(ee,ff,bb);
let df(ra(ee,ff,bb),fx)  =  (b/c)*ab(ex,fx,bx)/ra(ee,ff,bb);
let df(ra(ee,ff,bb),fy)  =  (b/c)*ab(ey,fy,by)/ra(ee,ff,bb);
let df(ra(ee,ff,bb),fz)  =  (b/c)*ab(ez,fz,bz)/ra(ee,ff,bb);
let df(ra(ee,ff,bb),bx)  = -ab(ex,fx,bx)/ra(ee,ff,bb);
let df(ra(ee,ff,bb),by)  = -ab(ey,fy,by)/ra(ee,ff,bb);
let df(ra(ee,ff,bb),bz)  = -ab(ez,fz,bz)/ra(ee,ff,bb);
let df(ab(ex,fx,bx),ex)  = a/c;
let df(ab(ey,fy,by),ey)  = a/c;
let df(ab(ez,fz,bz),ez)  = a/c;
let df(ab(ex,fx,bx),fx)  = b/c;
let df(ab(ey,fy,by),fy)  = b/c;
let df(ab(ez,fz,bz),fz)  = b/c;
let df(ab(ex,fx,bx),bx)  = -1;
let df(ab(ey,fy,by),by)  = -1;
let df(ab(ez,fz,bz),bz)  = -1;
let df(ab(ex,fx,bx),ey)  = 0;
let df(ab(ex,fx,bx),ez)  = 0;
let df(ab(ex,fx,bx),fy)  = 0;
let df(ab(ex,fx,bx),fz)  = 0;
let df(ab(ex,fx,bx),by)  = 0;
let df(ab(ex,fx,bx),bz)  = 0;
let df(ab(ey,fy,by),ex)  = 0;
let df(ab(ey,fy,by),ez)  = 0;
let df(ab(ey,fy,by),fx)  = 0;
let df(ab(ey,fy,by),fz)  = 0;
```

```
;  <WATTS>G090.04;10    WED 15-NOV-78 8:55AM

let df(ab(ey,fy,by),bx)  =  0;
let df(ab(ey,fy,by),bz)  =  0;
let df(ab(ez,fz,bz),ex)  =  0;
let df(ab(ez,fz,bz),ey)  =  0;
let df(ab(ez,fz,bz),fx)  =  0;
let df(ab(ez,fz,bz),fy)  =  0;
let df(ab(ez,fz,bz),bx)  =  0;
let df(ab(ez,fz,bz),by)  =  0;
let df(rq(ee,ff,bb),ex)  =  (a/d)*dq(ex,fx,bx)/rq(ee,ff,bb);
let df(rq(ee,ff,bb),ey)  =  (a/d)*dq(ey,fy,by)/rq(ee,ff,bb);
let df(rq(ee,ff,bb),ez)  =  (a/d)*dq(ez,fz,bz)/rq(ee,ff,bb);
let df(rq(ee,ff,bb),fx)  =  (b/d)*dq(ex,fx,bx)/rq(ee,ff,bb);
let df(rq(ee,ff,bb),fy)  =  (b/d)*dq(ey,fy,by)/rq(ee,ff,bb);
let df(rq(ee,ff,bb),fz)  =  (b/d)*dq(ez,fz,bz)/rq(ee,ff,bb);
let df(rq(ee,ff,bb),bx)  =(cc/d)*dq(ex,fx,bx)/rq(ee,ff,bb);
let df(rq(ee,ff,bb),by)  =(cc/d)*dq(ey,fy,by)/rq(ee,ff,bb);
let df(rq(ee,ff,bb),bz)  =(cc/d)*dq(ez,fz,bz)/rq(ee,ff,bb);
let df(dq(ex,fx,bx),ex)  =   a/d;
let df(dq(ey,fy,by),ey)  =   a/d;
let df(dq(ez,fz,bz),ez)  =   a/d;
let df(dq(ex,fx,bx),fx)  =   b/d;
let df(dq(ey,fy,by),fy)  =   b/d;
let df(dq(ez,fz,bz),fz)  =   b/d;
let df(dq(ex,fx,bx),bx)  =  cc/d;
let df(dq(ey,fy,by),by)  =  cc/d;
let df(dq(ez,fz,bz),bz)  =  cc/d;
let df(dq(ex,fx,bx),ey)  =  0;
let df(dq(ex,fx,bx),ez)  =  0;
let df(dq(ex,fx,bx),fy)  =  0;
let df(dq(ex,fx,bx),fz)  =  0;
let df(dq(ex,fx,bx),by)  =  0;
let df(dq(ex,fx,bx),bz)  =  0;
let df(dq(ey,fy,by),ex)  =  0;
let df(dq(ey,fy,by),ez)  =  0;
let df(dq(ey,fy,by),fx)  =  0;
let df(dq(ey,fy,by),fz)  =  0;
let df(dq(ey,fy,by),bx)  =  0;
let df(dq(ey,fy,by),bz)  =  0;
let df(dq(ez,fz,bz),ex)  =  0;
let df(dq(ez,fz,bz),ey)  =  0;
let df(dq(ez,fz,bz),fx)  =  0;
let df(dq(ez,fz,bz),fy)  =  0;
let df(dq(ez,fz,bz),bx)  =  0;
let df(dq(ez,fz,bz),by)  =  0;
let rtd*rtd = d;
let rtc*rtc = c;
out sam;
procedure ocent(d1);
begin d2 := sub(sinh(z)=zz+zz**3/6+zz**5/120+zz**7/5040+zz**9/362881,
        cosh(z)=1+ZZ**2/2+ZZ**4/24+ZZ**6/720+ZZ**8/40320+ZZ**10/3628800
    **,01);

d3 := sub(zz=2*c*r*rab,d2);
```

```
; <44 TTS>0010.34:10   WED 15-NOV-78 8:55AM

d4 := sub(abx=0,aby=0,abz=0,rab=0,d3);
return d4;
end;
comment*****************************************************************;
q1 := e***(-3*b*r*a(ee,ff)**2/c);
q22 := e***(-3*c*c*r*a(ee,ff,bb)**2/4);
q23 := e***(-d*r*q(ee,ff,bb)**2);
q24 := (3*b*i*r*d)/(r*c*c*r*a(ee,ff,bb));
q25 := sinh(2*d*r*a(ee,ff,bb));
q10 := (3*c*c*(q1)**2)/(4*cc**2)+q1)/(2*cc**2))-11*q3*q4*r**2*q5)/2;
Let d=c*cc*r*t=r*c*cc;
q220 := 3;
Let cc=3;
q221 := ff(q20,fx)/(2*b)$
q224 := ff(q20,fy)/(2*b)$
q227 := ff(q21,ex)/(2*a)$
q234 := ff(q20,ey)/(2*a)$
q237 := ff(q27,ez)/(2*a)$
comment*****************************************************************;
Let ra(ee,ff)=ref,ra(ee,ff,bb)=rab,ef(ex,fx)=efx,ef(ey,fy)=efy,ef(ez,fz)=efz,
        AB(EX,FX,BX)=ABX,AB(EY,FY,BY)=ABY,AB(EZ,FZ,BZ)=ABZ;

Let rd(ee,ff,bb)=rab,dg.ex,fx,bx)=abx,dg(ey,fy,by)=aby,dg(ez,fz,bz)=abz;
Let d=c*r*t=c;
q11 := 3;
Let cc=3;
Let sinh(2*c*r*a)=sinh(2*c*r*rab)=cosh(2*c*r*rab)=cosh(z);
q12 := sub(efx=0,efy=0,efz=0,q11);
sub(sinh(z)=z+z**3/6+z**5/120,cosh(z)=1+z**2/2+z**4/24+z**6/720,q12);
saveas q16;
suczz=2*c*r*rab,q16);
save q17;
q28 := sub(abx=0,aby=0,abz=0,rab=0,q17);
q228 := sub(efx=0,efy=0,efz=0,q27);
q229 := ocunt(q28);
q232 := sucent(efx=0,efy=0,efz=0,q31);
q235 := sucent(efx=0,efy=0,efz=0,q34);
q236 := ocunt(q35);
q238 := sucent(efx=0,efy=0,efz=0,q37);
q239 := ocunt(q38);
shut save;
off nat;
factor i,c;
out qfn;
write "comment (s,s)";
q20 := q11;
q12 := q12;
q18 := q19;
write "comment  (s,ox)";
```

```
;  <WATTS>0009.34;10    WED 15-NOV-78 8:55AM

q21 := q21;
write "comment   (s,py)";
q24 := q24;
write "comment   (s,pz)";
q27 := q27;
q28 := q28;
q29 := q29;
write "comment   (px,px)";
q31 := q31;
q32 := q32;
q33 := q33;
write "comment   (py,py)";
q34 := q34;
q35 := q35;
q36 := q36;
write "comment   (pz,pz)";
q37 := q37;
q38 := q38;
q39 := q39;
write "end";
shut qfn;
on nat;
```